ΕΘΝΙΚΟ ΜΕΤΣΟΒΙΟ ΠΟΛΥΤΕΧΝΕΙΟ
ΣΧΟΛΗ ΧΗΜΙΚΩΝ ΜΗΧΑΝΙΚΩΝ
ΕΡΓΑΣΤΗΡΙΟ ΤΕΧΝΟΛΟΓΙΑΣ ΑΝΟΡΓΑΝΩΝ ΥΛΙΚΩΝ

Catalytic hydrogenation of carbon dioxide via plug-flow dielectric barrier discharge (DBD) plasma reactor

Zoi Asteriou

Supervisor: Christos Argirusis, Prof. NTUA

Athens, 2024

Περίληψη

Η παρούσα διπλωματική εργασία εστιάζει στην καταλυτική υδρογόνωση του διοξειδίου του άνθρακα (CO_2) χρησιμοποιώντας τόσο θερμικές μεθόδους όσο και μεθόδους πλάσματος. Οι καταλύτες που χρησιμοποιήθηκαν για αυτή την διπλωματική εργασία ήταν: CeO_2, CeO_2/CuO 10%, και CeO_2/CuO 20% και ο κύριος στόχος ήταν η αξιολόγηση και σύγκριση της αποτελεσματικότητάς τους, της εκλεκτικότητας τους σε χημικά πολύτιμα προϊόντα και της σταθερότητά τους.

Η έρευνα ξεκινά με τη διερεύνηση του θεωρητικού υποβάθρου των εκπομπών CO_2. Έπειτα, αναλύεται η αντίδραση υδρογόνωσης CO_2 και τα πιθανά προϊόντα της. Αφού παρατέθηκαν τα πιθανά προϊόντα της αντίδρασης, στη συνέχεια αναλύθηκαν οι μη ευγενείς καταλύτες οι οποίοι χρησιμοποιήθηκαν στην αντίδραση. Πιο συγκεκριμένα είναι το οξείδιο του δημητρίου (CeO_2) και το οξείδιο του δημητρίου με πρόσμειξη οξειδίου του χαλκού (CeO_2/CuO 10%, και CeO_2/CuO 20%).

Τα υλικά που χρησιμοποιήθηκαν στα πειράματα περιλαμβάνουν αέριο διοξείδιο του άνθρακα (CO_2), υδρογόνο (H_2) και ήλιο (He) καθώς και τους καταλύτες που έχουν ήδη αναφερθεί. Τα πειράματα χωρίστηκαν σε δύο κατηγορίες: θερμικά και με πλάσμα. Για τα θερμικά πειράματα χρησιμοποιήθηκε ένας φούρνος ως πηγή ενέργειας, ενώ για τα πειράματα πλάσματος χρησιμοποιήθηκε ένας αντιδραστήρας εκκένωσης διηλεκτρικού φράγματος (DBD).

Τα πειράματα τα οποία πραγματοποιήθηκαν με τη θερμική μέθοδο διεξήχθησαν σε διάφορες θερμοκρασίες προκειμένου να βρεθεί η θερμοκρασία που ξεκινάει η αντίδραση με τον κάθε καταλύτη. Το CeO_2 έδειξε ελάχιστη μετατροπή του CO_2 σε χαμηλές θερμοκρασίες, με σημαντική αύξηση της μόνο στους 500 °C. Η προσθήκη CuO στο CeO_2 βελτίωσε σημαντικά την καταλυτική συμπεριφορά, με το CeO_2/CuO 20% να επιτυγχάνει τα υψηλότερα ποσοστά μετατροπής του CO_2, ακόμη και σε χαμηλότερες θερμοκρασίες. Αυτή η βελτίωση αποδίδεται στο συνεργιστικό αποτέλεσμα του CuO, το οποίο δημιουργεί περισσότερες ενεργές θέσεις για την προσρόφηση του CO_2.

Στα πειράματα πλάσματος, η μετατροπή του CO_2 ήταν σταθερή ως συνάρτηση του χρόνου. Η μεταβλητή που εξετάστηκε ήταν η μετατροπή CO_2 συναρτήσει της τάσης. Στα πειράματα χωρίς καταλύτη, η μετατροπή του CO_2 αυξήθηκε με την τάση, φτάνοντας έως και 16% στα 10 kV. Η προσθήκη των καταλυτών βελτίωσε σημαντικά τη μετατροπή και τη σταθερότητα του πλάσματος. Το CeO_2/CuO 20% έδειξε για άλλη

μια φορά την καλύτερη καταλυτική απόδοση επιτυγχάνοντας 26% μετατροπή στα 10 kV. Η μέθοδος πλάσματος αποδείχθηκε ότι είναι μια πολύ αποτελεσματική μέθοδος, καθώς σε θερμοκρασία δωματίου, μπορέσαμε να επιτύχουμε μια επαρκή μετατροπή.

Μια συγκριτική ανάλυση των μεθόδων αποκάλυψε ότι η υδρογόνωση CO_2 με πλάσμα προσφέρει περισσότερα πλεονεκτήματα, ιδιαίτερα όσον αφορά την ενεργειακή απόδοση και την καταλυτική δραστηριότητα σε χαμηλότερες θερμοκρασίες. Ο καταλύτης CeO_2/CuO 20% φάνηκε να έχει την καλύτερη απόδοση και στις δύο μεθόδους.

Το τελευταίο μέρος των πειραμάτων ήταν οι δοκιμές σταθερότητας του καλύτερου καταλύτη CeO_2/CuO 20%. Αρχικά, ο καταλύτης ανοίχθηκε με H_2 στους 500°C και στη συνέχεια δοκιμάστηκε υπό συνθήκες πλάσματος στα 10 kV. Τα αποτελέσματα έδειξαν σταθερούς ρυθμούς μετατροπής CO_2 για εκτεταμένες περιόδους. Αυτό δείχνει ότι ο καταλύτης μπορεί να χρησιμοποιηθεί για μακροχρόνιες διεργασίες υδρογόνωσης CO_2 σε περιβάλλον πλάσματος.

Συνοψίζοντας, αυτή η μελέτη υπογραμμίζει τη σημασία των καταλυτών για την υδρογόνωση του CO_2. Η μελλοντική έρευνα θα μπορούσε να επικεντρωθεί στην εύρεση των βέλτιστων παραμέτρων του πλάσματος, όπως η τάση, οι ροές των αερίων, καθώς και η διερεύνηση νέων συνθέσεων καταλυτών. Μελλοντικές έρευνες θα μπορούσαν επίσης να διερευνήσουν εάν η προσθήκη επιπλέον CuO οδηγεί σε ακόμη καλύτερες μετατροπές. Επιπλέον, η μακροπρόθεσμη σταθερότητα του καταλύτη θα πρέπει να εξεταστεί περαιτέρω προκειμένου να εξακριβωθεί εάν μια τέτοια διαδικασία θα μπορούσε να χρησιμοποιηθεί σε μεγαλύτερη κλίμακα.

Abstract

The current thesis focuses on the catalytic hydrogenation of carbon dioxide (CO_2) using both thermal and plasma methods. The catalysts used for this thesis were: CeO_2, CeO_2/CuO 10%, and CeO_2/CuO 20% and the main focus was to assess their efficiency, selectivity to valuable products and stability.

The thesis begins by exploring the theoretical background of CO_2 emissions and introducing the CO_2 hydrogenation reaction and its possible pathways. After discussing the possible products that can be acquired by the reaction, then the non-noble catalysts that facilitated the reaction were analyzed. Particularly, cerium oxide (CeO_2) and copper-doped cerium oxide (CeO_2/CuO 10%, and CeO_2/CuO 20%).

The materials used in the experiments include CO_2, hydrogen (H_2), and helium (He) gases, along with the catalysts that have already been mentioned. The experiments were separated into two categories: thermal and plasma. For the thermal experiments, a conventional oven was used as a source of energy, while for the plasma experiments, a plug-flow dielectric barrier discharge (DBD) plasma reactor was used.

For the thermal method, experiments were conducted in various temperatures, starting from 20 °C and reaching 500 °C, to determine the temperature at which each catalyst becomes active, and the reaction takes place. CeO_2 was the weakest catalyst since it demonstrated minimal CO_2 conversion at lower temperatures. The reactants started to convert at 500 °C. The introduction of CuO to CeO_2 significantly enhanced catalytic performance. CeO_2/CuO 20% achieves the highest CO_2 conversion rates, at the lowest temperatures (300 °C). This improved catalytic behavior is because of the synergistic effect of CuO, which creates more active sites for CO_2 adsorption and improves the reduction process.

For the plasma experiments, the CO_2 conversion was stable as a function of time. The variable that was examined was how the CO_2 conversion was affected by the different applied voltages. Without a catalyst, CO_2 conversion increased with voltage, reaching up to 16% at 10 kV. The addition of the catalysts significantly improved the conversion and stability of plasma. CeO_2/CuO 20% showed once again the best catalytic performance achieving 26% conversion at 10 kV. The plasma method was proved to be a very efficient method since in room temperature, we were able to accomplish an adequate conversion.

A comparative analysis of the thermal and plasma methods revealed that plasma-assisted CO_2 hydrogenation offers distinct advantages, particularly in terms of energy efficiency and catalytic activity at lower temperatures. The CeO_2/CuO 20% catalyst appeared to have the best performance in both methods.

The last part of the experiment was the stability tests on the CeO_2/CuO 20% catalyst. Firstly, the catalyst was reduced with H_2 at 500°C and then it was tested under plasma conditions at 10 kV. The results showed consistent CO_2 conversion rates over extended periods. This shows that the catalyst can be used for long-term plasma-assisted CO_2 hydrogenation processes.

To sum up, this study highlights the importance of catalysts in CO_2 utilization. Future research should focus on finding the optimal plasma parameters such as voltage, gas flow ratios as well as exploring new catalyst compositions. Future research could also investigate whether the additional loading of CuO results in even better conversions. Additionally, the long-term stability of the catalyst should be further examined in order to conclude whether such a process could be scaled up.

Concluding, this thesis emphasizes how the catalytic hydrogenation of CO_2 under thermal and plasma sources, combined with non-noble catalysts can efficiently convert a pollutant to chemically valuable products.

Contents

1. Introduction

1.1. Environmental, economic, and social effects of CO_2 emissions

The climate has a great impact on the environment, economy and society of any region. Changes in light, temperature, humidity and gases play a role in influencing cycles, wind patterns, rainfall distribution and plant growth. While technological advancements have brought benefits to humanity they have also contributed to the depletion of resources and disrupted the balance of the environment. The heavy reliance on fuels, deforestation, desertification, soil degradation, rapid industrialization, and increased use of automobiles have altered conditions over time resulting in problems such as the greenhouse effect, ozone layer depletion and global warming. [1]

The ozone layer is often referred to as Earth's "umbrella". It is situated in the stratosphere, and it serves as a shield with a concentration of ozone (O_3) that absorbs 94-99% of sunlight harmful to life, on Earth's surface. Currently, ozone depletion is a concern attributed mainly to chlorofluorocarbons causing this breakdown. Moreover, the thinning of the ozone layer is closely linked to carbon dioxide emissions primarily associated with warming. Carbon dioxide (CO_2) methane (CH_4) and chlorofluorocarbons (CFCs) are the greenhouse gases that play a role in the depletion of the ozone layer.

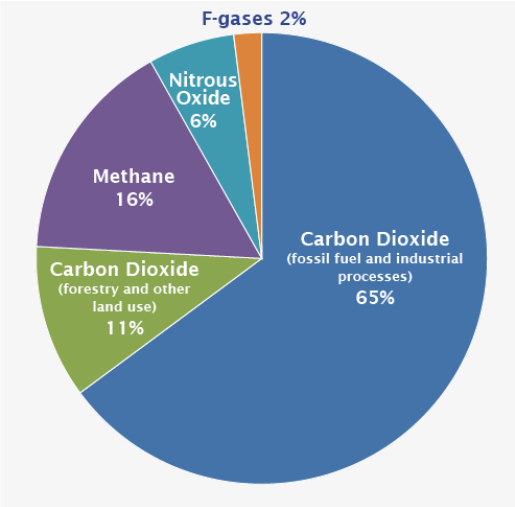

Figure 1: Global emission [2]

Global emissions of pollutants causing ozone degradation and the greenhouse effect are shown in Figure 1.

- Carbon dioxide (CO_2) originates from fossil fuel combustion. Additionally, deforestation, agriculture and soil degradation contribute to CO_2 emissions.
- Methane (CH_4) emissions mostly derive from agriculture and biomass burning.
- Nitrous oxide (N_2O) emissions come from agricultural products like fertilizers and fossil fuel combustion.
- Fluorinated gases (F-gases), hydrofluorocarbons (HFCs), perfluorocarbons (PFCs) and sulfur Hexafluoride (SF6) originate from industrial processes and refrigerating systems.

Financial development plays a significant role in the energy consumption of each country and as a result CO_2 emission. Studies reveal that as the financial growth of a country increases, the total CO_2 emissions decrease.

Additionally, the influx in oil prices has important effects on the economy. Some studies indicate that higher oil prices have a short-term positive effect on CO_2 emissions, but long term, they can be detrimental. The connection between climate change, energy use, and sustainable economic growth has captured the interest of many researchers. Some believe that environmental regulations and policies might restrict production capabilities and potentially slow down long-term economic growth.[3] Some countries may experience little to no impact on emissions from oil price changes. While the relationship between prices and emissions is yet to be established, higher oil prices may lead to a reduction in CO_2 emissions.[4]

1.2. CO_2 capture

Carbon dioxide (CO_2) capture and utilization (CCU) are gaining increasing attention because of the multiple advantages they offer. Primarily, capturing and utilizing carbon dioxide is crucial for global warming moderation and its detrimental effects on the environment and humanity. Furthermore, studies have shown that carbon dioxide could be used as feedstock to produce valuable fuels and chemicals. The most desirable path for CO_2 conversion is its dissociation into CO, which can later on be converted into various fuels and chemicals. The conversion of CO_2 has been proven to have extremely high activation energy. If CO_2 were to be dissociated thermally it would demand temperatures exceeding 1200 °C. This reaction is thermodynamically unfavorable, resulting in high energy demand.

As mentioned, CO_2 conversion is a reaction that takes place in extreme conditions. Non-thermal plasma (NTP) has been gaining attention nowadays as a promising alternative to the thermal conversion of CO_2. Non-thermal plasma does not require high pressure or temperature for CO_2 to be activated because of its non-equilibrium nature. Furthermore, NTP can be instantaneously switched on and off, making it more flexible and compatible with renewable energy sources.

Despite its promising prospects, NTP is typically not used for industrial-scale applications because of its low selectivity. On the other hand, combining non-thermal plasma with a catalyst can drastically improve selectivity, CO_2 conversion and energy efficiency. Thus, designing bespoke catalysts with structural and compositional properties is crucial for CO_2 conversion. Catalysts have been proven to influence the local electric field, change plasma discharge characteristics, and provoke micro-discharges within porous structures. Simultaneously, non-thermal plasma can significantly affect catalysts by modifying their microscopic structure, metal dispersion, and chemical states.[5]

2. Theoretical Framework

2.1. Reaction Mechanisms

Hydrogen serves as a high-energy element facilitating CO_2 conversion, yielding products categorized into fuels and chemicals. The rising demand for fuels results in high energy consumption, yet fossil fuels are non-renewable, so oil prices gradually increase. Therefore, renewable energy sources are widely investigated. Products of CO_2 hydrogenation like methanol, dimethyl ether (DME), and hydrocarbons are excellent fuels for internal combustion engines. Furthermore, methanol and formic acid serve as raw materials and intermediates in various chemical industries. Despite these benefits challenges surrounding hydrogen production, storage, and transportation need to be addressed. Hydrogen can be sourced from existing fossil fuel reservoirs, primarily natural gas, or through water splitting via electrolysis or other methods for chemical CO_2 recycling. [6]

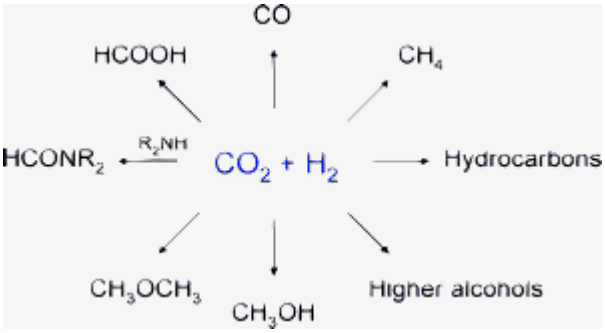

Figure 2: Catalytic hydrogenation of CO_2 [7]

In recent years, the hydrogenation of CO_2 has attracted significant attention due to its essential role in fields like catalysis, surface science, biology, nanoscience, nanotechnology, and environmental science. Both homogenous and heterogeneous catalysts have been employed for this purpose. Even though homogenous catalysts show satisfactory activity and selectivity, challenges arise in their recovery and regeneration. On the other hand, heterogeneous catalysts exhibit various advantages in stability, separation, reuse and reactor design resulting in lower costs making them more suitable for large-scale production. Numerous comprehensive reviews have explored CO_2 conversions and catalytic hydrogenation, primarily focusing on general applications and heterogeneous catalysis. [8],[9]

Catalytic hydrogenation of CO_2 can result in various products as depicted in Figure 2. The most common reactions are the following: [10]

$$CO_2 + H_2 \leftrightarrow CO + H_2O,\ \Delta H_{298K} = 41.2\ , kJ\ mol^{-1} \quad (1)$$

$$CO_2 + 4H_2 \leftrightarrow CH_4 + 2H_2O,\ \Delta H_{298K} = -165\ , kJ\ mol^{-1} \quad (2)$$

$$CO_2 + 3H_2 \leftrightarrow CH_3OH + H2O, \Delta H_{298K} = -49.2\ , kJ\ mol^{-1} \quad (3)$$

Reaction (2), CO_2 to CH_4, is the most common hydrogenation pathway because of the clean energy carrier methane. The reaction is highly exothermic, meaning that CH_4 selectivity increases at low temperatures and high pressures. The hydrogenation of CO_2 to CO occurs with the endothermic reaction (1) called reverse water-gas shift (RWGS). [11]

RWGS is deemed to be one of the most promising pathways for the hydrogenation of CO_2 to CO. It produces a gas mixture containing carbon monoxide (CO) and hydrogen (H_2), also known as synthesis gas or syngas which serves as a great feedstock for the synthesis of other chemicals and fuels contributing to the Circular Economy. [12] Syngas is widely used in industrial refineries for processes such as Fischer-Tropsch and the production of alcohols, mainly methanol, which is one of the most sold products in the world. [13]

RWGS reaction is characterized by its equilibrium nature, which is favored in higher temperatures due to its endothermic properties. Compared to other CO_2 conversion pathways, such as methanation and reforming reactions, RWGS has a brief contact time.

The obtained products from CO_2 hydrogenation are correlated with the reaction temperature. For example, methane (CH_4) is the main product within the temperature range of 100-700 °C. Carbon monoxide (CO) becomes the main product above 700 °C. [14]

Even though CO_2 methanation has been proven to be achievable even at low pressures and temperatures, it presents technological challenges due to CO_2 high stability. Industrial processes like power generation and refineries release large amounts of CO_2 which can be captured using absorption technologies. As mentioned, methane is the main product of CO_2 hydrogenation at temperatures between 100-700 °C. [15]

2.2. Catalysis

For a chemical reaction to occur, the reactants' bonds need to be rearranged as the bonds in the products are different to those in the reactants. The bond rearrangement is named the transition state and is the slowest step in the reaction.

$$\text{Reactant} \rightleftarrows \text{Transition State} \rightleftarrows \text{Product}$$

The energy required to form the transition state is called activation energy also known as Ea. Reactants with kinetic energy higher than the activation energy at a given temperature convert to products, while those with lower kinetic energy do not. Thus, when the activation energy is low, more reactants can convert to products.

Catalysis is the increase in the rate of a chemical reaction due to a catalyst. A catalyst is a substance that alters the rate of a chemical reaction without being consumed. It can speed up a reaction without modifying the reaction equilibrium. The main function of the catalyst is to reduce the activation energy so that a larger number of molecules can react. Figure 3 illustrates the energy activation (Ea) demand for a reaction without a catalyst and with a catalyst.

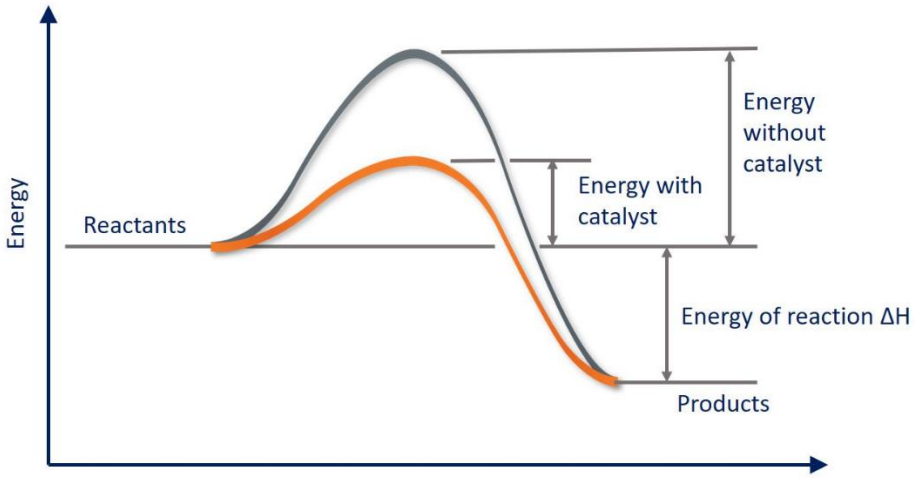

Figure 3: Comparison of the transition state with and without catalyst. [16]

Carbon dioxide is a stable molecule, thus a high amount of energy is required for carbon dioxide hydrogenation. In previous years, noble metals, like palladium (Pd), aurum (Au), and ruthenium (Ru) were used as catalysts for the hydrogenation reaction. However, noble metal catalysts are expensive and are not broadly available which makes it impossible to use them on an industrial scale.[17],[18], [19] Nowadays, much research

has been conducted in substituting noble metals with non-noble metals, as the latter display high stability and high activity.[20]

The main characteristics of a catalyst are the surface area, selectivity, activity and life span: [21]

- Surface: Catalytic reactions appear when a fluid and a solid interface, so for a high reaction rate, a large surface area is essential. This is often accomplished by creating a porous catalyst, which can impact its activity greatly. The pore structure can permit entrance to only certain molecules or regulate the residence times of numerous molecules, thereby influencing selectivity. To achieve a large surface area, on which the active catalyst is evenly allocated, a high specific surface area substrate can be used

- Selectivity: Selectivity denotes to a catalyst's ability to selectively enhance the production of a specific product.

- Activity: Typically measured in moles of product produced per unit mass of catalyst, this is perhaps the most crucial characteristic of a catalyst. The active centers of the solid catalyst bind the reactants and interact with them, leading to bond cleavage. Reactant binding presents itself through physical surface assimilation and chemisorption. The reaction rate does not get significantly affected by the Physical adsorption which decreases rapidly with increasing temperature. Contrary to chemisorption, this relies on strong valence forces similar to chemical bonds, significantly affecting the reaction rate. The adsorption of reactants by the catalyst's active centers must be strong enough for successful activation but not so strong that it prevents the product from being released, to achieve optimal activity

- Lifetime: Lifetime is characterized by the decline in catalyst activity over time. Catalyst deactivation can appear due to thermal aging, poisoning, contamination, or carbon deposition. [22], [23]

Modern catalyst systems have a specific structure, usually consisting of two elements: the carrier (or substrate) and the active metal in order to achieve the desired characteristics. The active metal catalyzes the reactions, while the carrier which is a less active substance,

is used to increase the specific surface area and improve the mechanical strength of the catalyst. Common carrier materials include aluminum oxide (Al_2O_3), cerium oxide (CeO_2), and silicon oxide (SiO_2).

Besides the increase of the specific surface area, in order to facilitate electron transfer, or form chemical bonds, which affects the catalyst's physicochemical properties, carriers have to merge with the active phase by changing its dispersion. Other benefits of using a substrate include reduced sensitivity to poisoning and improved heat management, which helps avoid pyro-agglomerates caused by local hot spots. In order to achieve the desired result while minimizing costs and energy requirements, it is essential to choose the right combination of carrier and active metal. [25]

2.3. CeO_2 catalyst

Cerium oxide or CeO_2 is a versatile catalyst that has been gaining attention in the last years due to its valuable properties such as improved thermal stability, high oxygen storage capacity, and oxygen mobility render. Unlike other elements in the lanthanide series, cerium can co-exist in both trivalent (Ce^{3+}) and tetravalent (Ce^{4+}) states. Cerium oxide's ability to switch easily between states makes it a perfect catalyst. This catalytic activity is used in hydrogen production, purification, and removing carbon monoxide from car exhaust. The tetravalent state of ceria is more stable, making it ideal for oxygen storage and transport. CeO_2 also finds use in oxygen-resistant materials, sensors, UV absorbers, light-harvesting devices, displays, silicon wafer buffers, nanomedicine, and tissue engineering. [26], [27], [28]

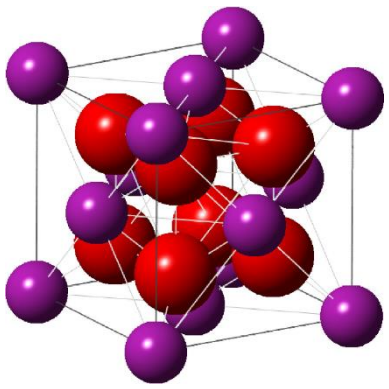

Figure 4: Cerium oxide structure [24]

Ceria is a key factor in many catalytic applications. For some, like fuel cells, CeO_2-based materials are almost market-ready. For others, such as reforming processes, photocatalysis, water-gas shift reactions, thermochemical water splitting, and organic reactions, ceria holds great future potential. As we learn more about CeO_2 through new techniques and theories, we

can better predict its behavior and applications. CeO_2 has a cubic fluorite-type in fcc arrangement as shown in Figure 4. [29]

Several articles have revealed that by combining CeO_2 with transition metals through various structural and surface functionalizing techniques, the catalytic performance drastically improves. The new catalysts are not only cost-effective but also highly efficient. [30], [31]

2.3.1. Catalytic Applications of CeO_2 Beads

- CO Oxidation: Nanostructured CeO_2 catalysts demonstrate assuring results for CO oxidation, which is vital for applications like automobile exhaust purification and fuel cells. Ce-Cu hybrids, such as $CuOx/CeO_2$, are especially effective due to the stabilization of Cu(I) by CeO_2, boosting catalytic activity. Various nanostructures such as nanorods and core-shell configurations have been created in order to improve low-temperature CO oxidation efficiency by increased surface defects and optimized interfaces. [32]

  Key Catalysts for CO Oxidation: $CuOx/CeO_2$ Nanorods: enhances activity due to surface defects. CuO/CeO_2 Core-Shell Nanostructures: Increases stability and catalytic performance. Co-Doped CeO_2 Nanotubes: Improves surface defect sites and redox properties. [33], [34], [35]

- NOx Destruction: CeO_2-based catalysts are essential in breaking down hazardous nitrogen oxides (NOx) from industrial emissions. A CuO/CeO_2 catalyst, mostly in the form of nanorods, establishes high activity because of their surface properties, encouraging oxygen mobility. Furthermore, CeO_2-based SCR catalysts, like NiO/CeO_2, effectively decrease NO_x emissions at low temperatures by converting NO_x to harmless nitrogen gas using reducing agents such as NH_3 or CO. Key Catalysts for NOx Destruction: CuO/CeO_2, Nanorods: High activity due to high-energy surface planes, NiO/CeO_2 NRs: Effective for NH_3-SCR of NO at low temperatures.

- Steam Reforming: CeO_2 boosts hydrogen production via steam reforming of methanol (SRM), a process for generating clean energy. CuO/CeO_2 catalysts,

enhanced with Cu content up to 70%, show increased activity because of improved distribution and durability of the Cu-active phase. Incorporating additional elements such as ZnO can further enhance the catalyst's morphology and improve its performance in hydrogen production. Key Catalysts for Steam Reforming: CuO/CeO_2 Composites: Optimal Cu content at 70% for SRM, ZnO-Promoted CuO/CeO_2: Improved morphology and hydrogen production efficiency.

2.4. CuO/CeO_2 catalyst

Copper oxide also known as CuO has been rapidly gaining attention during the past years due to its valuable properties such as soot oxidation, steam reforming, low-temperature oxidation, water gas shift (WGS) reaction, and dimethyl ether synthesis (DME). The combination of cerium oxide and copper oxide catalysts are emerging as a cost-effective substitute for noble metal catalysts due to their ability to activate oxygen. The CuO/CeO_2 is a catalyst with many oxygen vacancies enhancing the catalyst's redox ability and lattice oxygen. The key factor to the perfect catalyst is the ability to facilitate the copper atoms in changing their valences and to supply suitable oxygen atoms. [37], [38]

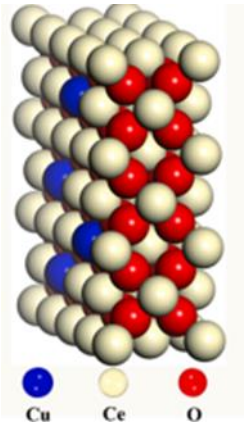

Figure 5: CuO/CeO_2 structure [36]

Recently, CuO/CeO_2 catalysts originating from metal-organic frameworks (MOFs) have gained attention due to their excellent specific surface area, abundance of functional groups, and tunable pore sizes. The MOF structure and moderate Cu loading lead to a satisfying Cu dispersion and strong redox ability of CuO/CeO_2. [39] The catalyst can be stabilized with thermal treatment conditions which greatly impact the surface area, dispersion and crystallite size. More specifically the concentration of active species in CuO/CeO_2 catalysts is linked to the annealing temperature with dispersion determined by the decomposition of organic ligands. [40] Furthermore, CuO/CeO_2 derived from Metal-Organic Frameworks demonstrate excellent catalysis due to the plethora of oxygen vacancies that provide extra absorption.

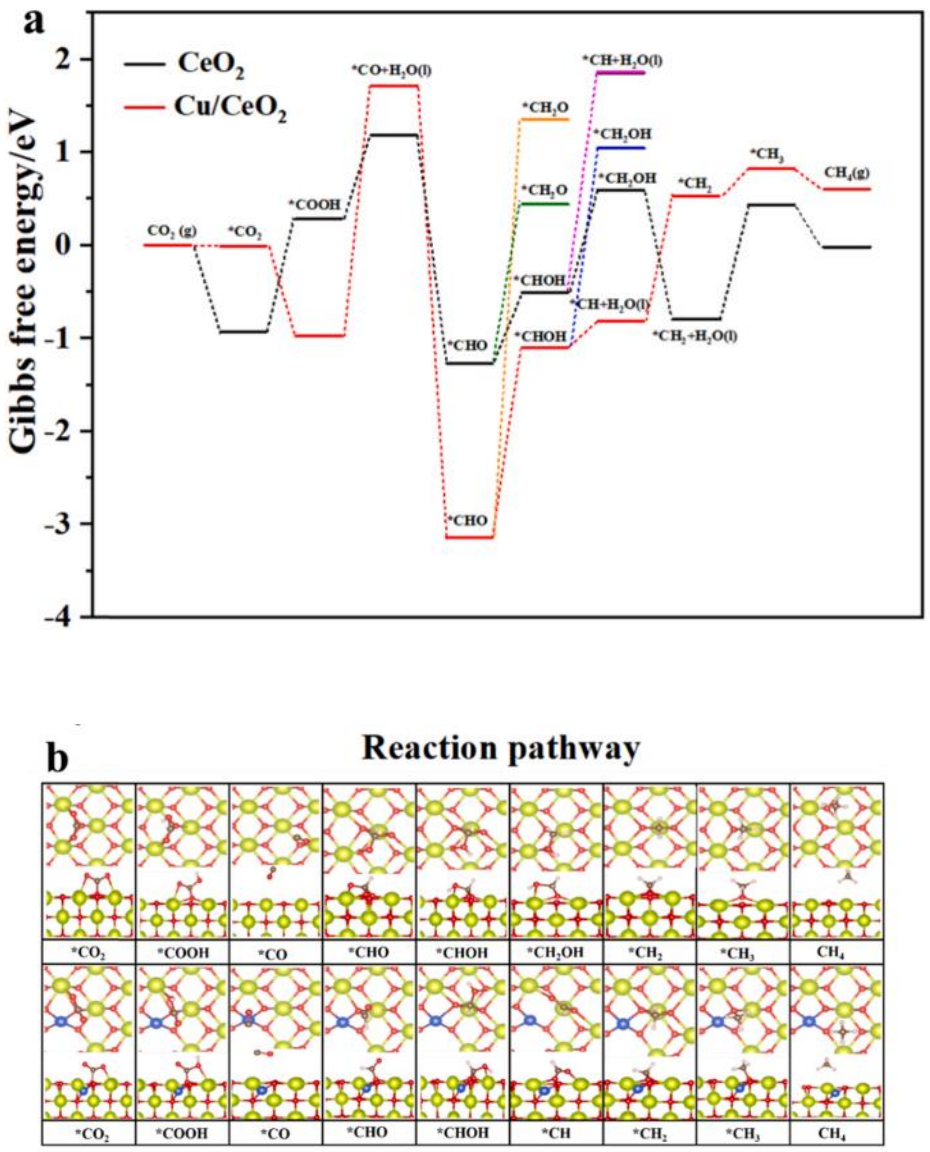

Figure 6:(a) Free energy diagrams of the optimal reaction pathway, and (b) corresponding configurations on CeO_2 (above) and Cu/CeO_2 (below) catalysts. [41]

Figures 6a and 6b describe how CO_2 molecules are absorbed and activated on the surfaces of pure CeO_2 and CuO/CeO_2 catalysts. As shown in Figure 6a, the absorbed CO_2 molecule undergoes the first hydrogenation step to give *COOH intermediate. As shown in the diagram the free energy barrier is negative for the CuO/CeO_2 catalyst indication that the reaction is exothermic and thermodynamically feasible. On the other hand, the reaction is challenging for pure CeO_2. CeO provide absorption sites for CO_2 molecule, thus, CuO

optimizes the absorption by reducing the energy absorption, as shown in Figure 6b. In summary, the optimal pathway for CH_4 production is $*CO_2 \rightarrow *COOH \rightarrow *CO \rightarrow *CHO \rightarrow *CHOH \rightarrow *CH_2OH \rightarrow *CH_2 \rightarrow *CH_3 \rightarrow CH_4$ on CeO_2, and $*CO_2 \rightarrow *COOH \rightarrow *CO \rightarrow *CHO \rightarrow *CHOH \rightarrow *CH \rightarrow *CH_2 \rightarrow *CH_3 \rightarrow CH_4$ on Cu/CeO_2. To sum up, doping CuO into the CeO_2 surface lowers the reaction energy barrier making the CO_2 hydrogenation more efficient. [42]

2.5. Plasma

Plasma is the fourth and most abundant state of matter, and exhibits widespread presence across the world, particularly prominent in intergalactic regions. It serves as an electrically neutral medium comprising unbound negative and positive charged particles, a state achieved through the application of electromagnetic field reinforcement to air and various gaseous compositions, along with the heating of compressed air or inert gases to generate ions. There is great interest among scholars in the creation of artificial plasma and the exploration of its potential societal benefits. [43]

The term plasma was first used by Langmuir in 1923 to describe the state of gases appearing in electric discharge experiments. Plasma is a gas that contains charged (positive ions and electrons) and neutral particles and that exhibit specific properties such as collective behavior and quasi-neutrality. The definition of quasi-neutrality is the equality between positively and negatively charged particles. Plasma is also characterized as the fourth state of matter. The most commonly used method for producing plasma for technological and technical applications is the electrical breakdown of a neutral gas through electrical discharges in the presence of an external electric field. [44]

An electric field can be created primarily by storing electric charges between two electrodes that produce electric potential distributions V. Electric charges are polarized through a dielectric (e.g., aluminum oxide), in which the positive charges within the dielectric are displaced in the direction of the electric field and the negative charges shift in the opposite direction. This small charge separation, or bias, reduces the electric field within the dielectric and limits the occurrence of sparks during electrical discharge. [45]

Many studies have shown that electrical gas discharges create the plasma. Plasma particles (neutral, positively and negatively charged) interact in various ways with each

other, with surrounding materials and the electric and magnetic fields present during the discharge. This multitude of particles and interactions makes electrical gas discharge a complex system that is not yet fully understood. The light electrons are heated by the applied electric field and activate the gas molecules by excitation, ionization and dissociation, creating the various types of ions, radicals and excited atoms and molecules and allowing chemical reactions to occur under mild conditions (ambient temperature and atmospheric pressure).

In nature, electrical discharges have been observed since early times with lightning, northern lights, etc. After electricity was discovered and understood, we were able to explain these phenomena. Now, with studies and observations, we can create electrical discharges ourselves. [46]

Gas electrical discharge can be created, as mentioned above, by directing electricity through a gas and to achieve these amounts of electrical charge must first be created and stored between two electrodes. There are several types of discharges depending on the voltage applied to the electrode gap and the current that can be sustained.
The movement in ordinary gases results only from the collisions between them because they are neutral, so there are no other external forces such as electromagnetic forces and gravity. On the contrary, in plasma, the movement of particles creates electric fields and currents which in turn create electromagnetic fields.

In plasma, the long-range Coulomb forces are the main forces that determine the motion of the particles in contrast to ordinary gases where the molecules react with each other mainly through short-range forces. Most systems in the universe such as stars, interstellar matter as well as the highest layers of the atmosphere are in a state of electrified gases where atoms are separated into positively charged ions and electrons. 99% of the matter in the universe is in plasma form while the 1% that resembles the state of matter on Earth is not in that form. It is therefore a highly reactive mixture, which makes it different from conventional gaseous mixtures.

Plasma is created by energizing gas until it ionizes. There are two main types of plasma, classified by electron temperature: non-thermal (cold) and thermal (hot). This distinction depends on factors like temperature, pressure and gas ionization.

2.5.1. Thermal (Hot) Plasma

Thermal plasma is a basic form of matter common throughout the universe, composed of equilibrium of negative ions and heavily charged particles at a homogeneous temperature. Electrochemical and electromagnetic mechanisms generate thermal plasma. [47] Furthermore, plasma antennas for beamforming display complex interactions among plasma elements, such as diverse scatterings from the edges of Argon Plasma cylinders and the transmission of electromagnetic waves on Argon Plasma.[48] These interactions collectively enable efficient beam radiation, formation, and scanning. Moreover, plasma-based ion implantation is an advanced technique used to apply thin coatings and alter surfaces.

2.5.2. Non-thermal Plasma (Cold Plasma)

Non-thermal Plasma (Cold Plasma) is characterized by its electron temperatures being much higher than those of heavily charged particles, operating beyond the confines of thermodynamic equilibrium. Typically, ion sources for generating non-thermal plasma include plasma generators that use electron cyclotron resonance and microwave ionization sources. Current research is focused on creating high-temperature plasma without gas collisions for use in space physics, inertial fusion, and magnetic fusion experiments. Vacuum microwave oscillators as ionization sources can be used to control the alterations in the frequency and power of radiation emitted by artificial plasma. [49]

The plasma gun technique for generating high-energy density plasma entails connecting electrodes to high current sources such as MARX generators or magnetic flux compression generators which enables the ionization of injected gas and the acceleration of ions through the Lorentz force mechanism, thereby facilitating the expulsion and subsequent flow of plasma.
Plasma technology is rapidly advancing to meet various industrial and commercial needs, playing a crucial role in metallurgical processes and creating nanotechnology tools for shaping antenna beams.[50]

Plasma is a high-efficiency, non-polluting method and one of the most promising approaches for the optimization of catalytical applications. As mentioned previously, plasma is an ionized gas that consists of ions, electrons, free radicals, excited molecules and neutrals. Plasma can be divided into two categories based on the gas temperature

(Tg): high-temperature plasma (i.e., Tg > 5000 K) and low-temperature plasma (i.e., T < 5000 K). Low- temperature plasma can be divided into nonthermal plasma (NTP or cold plasma) and thermal plasma. [51]

Non-thermal plasma or NTP can be characterized by different temperature scales and energy distributions of neutrality, ions, and electrons. Depending on the type of power, plasma discharge can be categorized into direct current (DC) plasmas, alternative current (AC) plasma, capacitively coupled plasmas (CCPs), inductively coupled plasmas (ICPs), microwave plasmas (MWPs), electron cyclotron resonance plasmas (ECRs), radio frequency discharge plasmas (RF) and pulse plasmas.

Another type of plasma characterization is the electrode configuration. Also, depending on the applied dielectric material or reactor structure, a wide range of plasma can be generated, including glow discharge (GDPs), corona discharge, dielectric barrier discharge (DBDs), gliding arc plasmas, and many others.

2.5.2.1. Corona Discharge (CD)

A corona discharge is created when a critical inhomogeneous electric field ionizes the gas surrounding a conductor. It is a self-sustaining discharge known for its luminous "corona effect," which is influenced by the geometry of the electrode (edges, wires, corners) [53] (Figure 7)

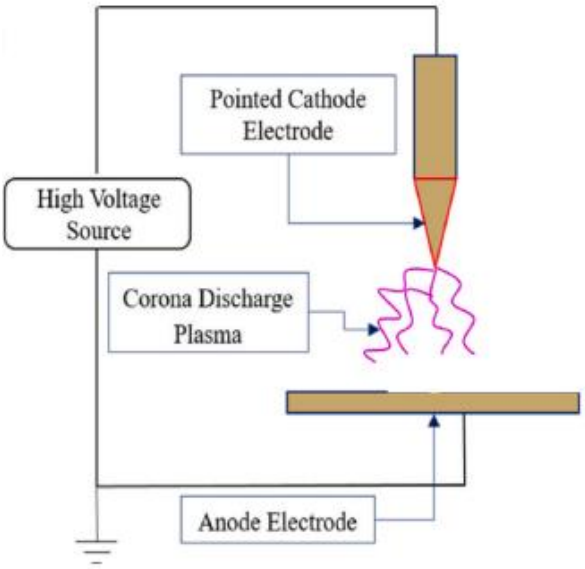

Figure 7: Corona Discharge [52]

2.5.2.2. *Gliding arc discharge*

Gliding arc plasma comprises of two symmetric electrodes located perpendicularly to the centric gas carrier source (Figure 8). In this type of plasma a higher voltage is applied between the two electrodes generating an arc that glides along the electrodes in the presence of dynamic flow. [54]

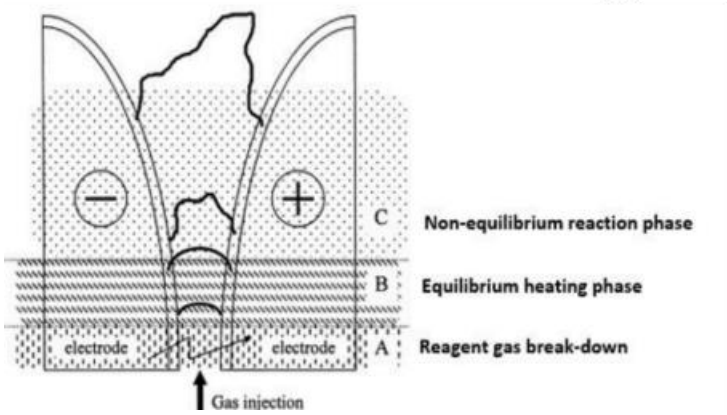

Figure 8: Gliding arc discharge [52]

2.5.2.3. *Glow discharge (GD)*

Glow discharge also known as GD is commonly known as low-pressure discharge (<10 mbar). GD is created when there is a potential difference between two electrodes

(Figure 9). The gas is ionized after the application of the voltage and as a result many cations and a free electron are created. Moreover, the free electrons are accelerated under the electric field, resulting in more and more ionization and excitation reactions. As a result of the excited particles there are many collisions and the

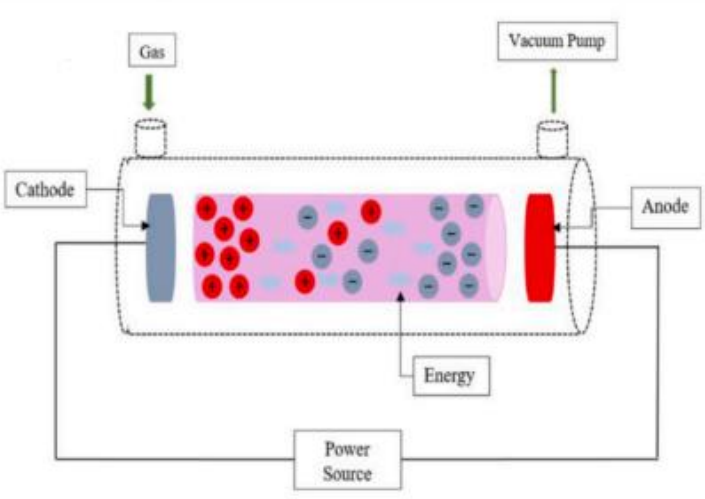

Figure 9: Glow discharge [52]

radiative deexcitation from higher energetic levels results in the apparition of plasma light "glow. [55]

2.5.2.4. Dielectric barrier discharge (DBD)

The dielectric barrier discharge (DBD) is one of the most popular non-thermal plasma technologies. Dielectric barrier discharge's advantages include its stability and its operating conditions (usually under normal atmospheric pressure and temperature). DBD plasma comprises of dielectric material such as ceramic, glass, plastic, or mica sandwiched between a high voltage (HV) electrode and a ground electrode (GE) (Figure 10). If a high voltage and frequency are applied, the gas inside is brought to its breakdown voltage, forming a discharge with a typical gap of 0.1–10 mm. DBD reactors' configurations vary depending on the electrode configuration, including surface DBD, planar DBD, and cylindrical DBD, as shown in Figure 11. [56], [57]

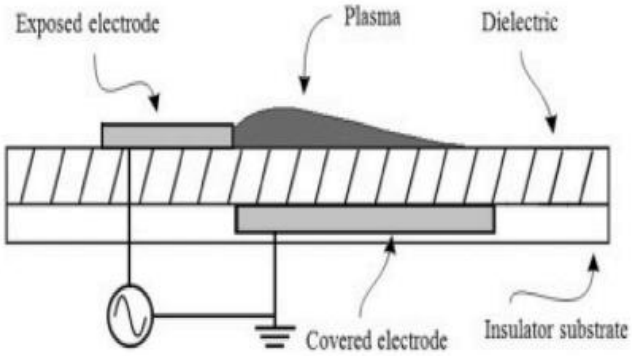

Figure 10: Dielectric Barrier Discharge [52]

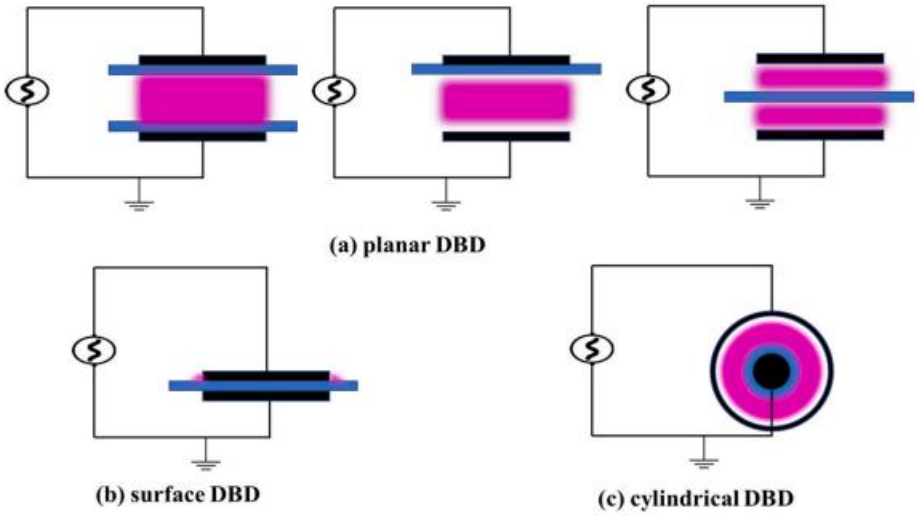

Figure 11: Different DBD configurations. [52]

Regarding CO_2 conversion, the DBD reactor is the most well-known non-thermal plasma production technology. Dielectric-barrier discharge is the electrical discharge between two electrodes separated by an insulating dielectric barrier. [58]
The DBD reactor generally operates at atmospheric pressure and low temperatures, and the typical energy level of high-energy electrons is between 1-10 eV. Since the dissociation of CO_2 requires an energy of 5.5 eV, it is therefore possible to convert it into value-added products. [59], [60]

A DBD is created by applying an electric field between two electrodes, at least one of which is covered by a dielectric barrier. The two electrodes can be parallel plates, but for CO_2 conversion, a cylindrical configuration in which the two electrodes are concentric cylinders is more suitable because it minimizes the amount of gas bypassing the plasma region Since the separation of CO_2 is mainly through electron bombardment, the basic plasma parameters and micro discharge properties determine the overall efficiency of the process. The plasma form in DBD reactors in CO_2-containing gases exhibits a filamentous form, i.e., the plasma progresses through transient and fine individual micro discharges (Micro Discharges-MDs). [61]

The simple design of DBDs also allows easy application of catalytic materials into the plasma to better control the selective production of value-added compounds.
Therefore, if the goal is the selective production of specific molecules, the plasma must be combined with catalysts and other reactants such as e.g. hydrogen or water, yielding so-called plasma catalysis. Most plasma catalysis studies indeed involve DBD plasma

reactors in a packed bed configuration, where the packing beads (a few millimetres in diameter) are typically coated with catalyst materials.

Non-thermal plasma's ability to operate in low temperatures and to initiate reactions beyond thermodynamic limits constitutes it one of the most revolutionary techniques for catalytic applications. However, sometimes in low temperatures, there is moisture residue which has a negative impact on catalytic reactivity. Hence, in most cases, heat treatment, hydrogen thermal reduction, or washing are placed after plasma treatment. Additionally, many researchers have shown that sometimes during NTP treatment a large number of hot spots are created on the surface of the catalyst, which increases the gas temperature and is beneficial to the activation of the catalyst. Furthermore, compared to thermal methods, the NTP method is a fast and simple process.

Non-thermal plasma ionizes the gas to create a highly reactive mixture and in combination with the catalyst the reaction takes place faster and more efficiently. Nowadays, NTP modifications have been gaining a lot of attention, yet, there is a huge lack of research. Few studies have discussed the modification mechanism of NTP and how it affects the catalyst properties. Many of these modifications include plasma doping, etching, redox and decomposition.

3. Materials and Methods

3.1. Materials

Three gases were used as reactants for the hydrogenation reaction:

1. Carbon Dioxide (CO_2)
2. Hydrogen (H_2)
3. Helium (He)

Three different catalysts were used in this study:

1. Cerium Oxide (CeO_2)
2. Cerium Oxide/Copper Oxide 10% (CeO_2/CuO 10%)
3. Cerium Oxide/Copper Oxide 20% (CeO_2/CuO 20%)

These catalysts were chosen due to their known efficiency in facilitating hydrogenation reactions. [62], [63], [64]

Reactor and Electrodes:

1. Reactor Material: Dense alumina (Al_2O_3)
2. DBD Electrodes: Stainless steel SS304

3.2. Methods

3.2.1. Experimental Setup

The experiments were conducted using two different energy sources: dielectric barrier discharge (DBD) plasma and a conventional oven. The aim was to compare the effectiveness of these energy sources in the catalytic hydrogenation of carbon dioxide.

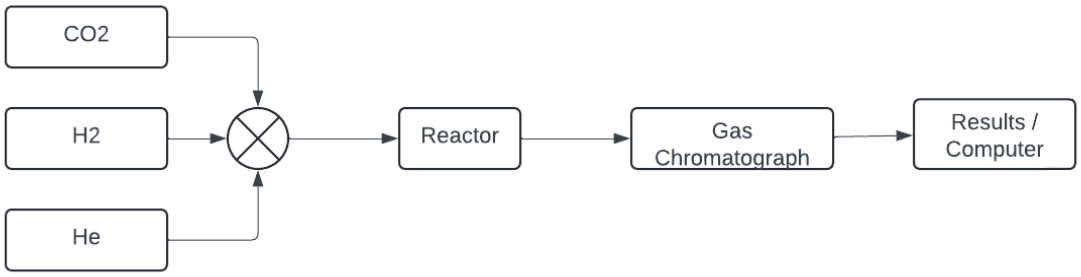

Figure 12: Experimental setup

3.2.2. Gas Feed Composition

The reactant gases were fed into the reactor in the following proportions:

- **Hydrogen (H_2)**: 2.08 ml/min
- **Carbon Dioxide (CO_2)**: 1.95 ml/min
- **Helium (He)**: 41.49 ml/min

These flow rates were maintained throughout the experiments to ensure consistent reactant availability and reaction conditions. The ratio of H_2 to CO_2 was 5, chosen based on established research indicating this ratio is optimal for effective hydrogenation reactions. [65], [66]

3.2.3. DBD Plasma Reactor

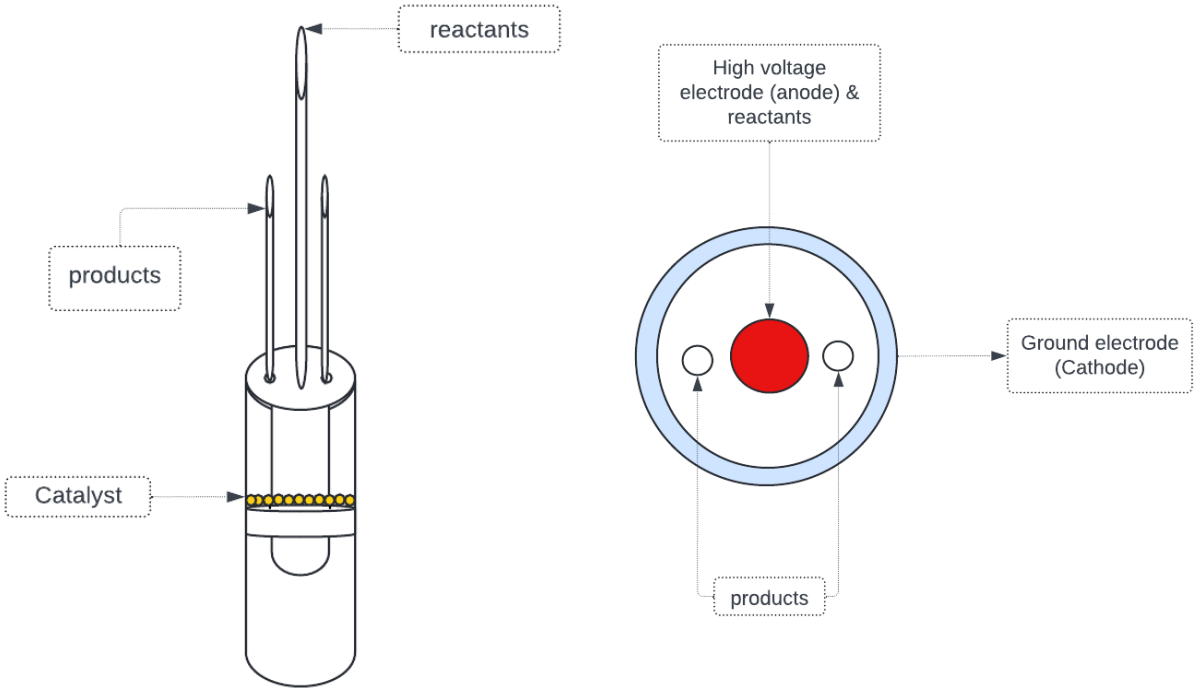

Figure 13: Cylindrical DBD plasma reactor

- **Reactor Design**: The DBD plasma reactor used was cylindrical with an external diameter of 2.5 cm, an internal diameter of 2.3 cm and a height of 10.1 cm.
- **High-voltage electrode (anode)**: Figure 13 illustrates the electrode configuration. The high-voltage electrode is made of stainless steel SS304 and has a diameter of 1.00 cm. It is connected to the high-voltage power supply (+).
- **Ground electrode (cathode)**: The ground electrode is made of stainless steel SS304 and is connected to the negative side of the power supply (-).
- **Catalyst Bed**: The catalyst bed had a height of 0.1 cm, corresponding to the approximate diameter of one catalyst bead, forming a single layer.
- **Reactor Volume**: The volume (V) of the reactor where the reaction took place was calculated using the formula:

$$V = \pi r^2 h \quad (1)$$

With a diameter of 1.3 cm, radius (r) of 0.65 cm and a catalyst bed height (h) of 0.1 cm, the volume was determined to be: V= 0.132665 cm^3

I. **Gas Hourly Space Velocity (GHSV)**: The GHSV was set at 20,352 h^{-1}.

$$GHSV = \frac{Q}{V} \quad (2)$$

The flow rate (Q) was set at 45 ml/min according to studies. [67], [68] The GHSV was calculated using the formula (1) and (2): GHSV=20,352 h^{-1}

3.2.4. Oven

- **Reactor Design**: The oven reactor used was cylindrical with a diameter of 1.295 cm. (Figure 14)
- **Catalyst Bed**: The catalyst bed had a height of 0.1 cm, corresponding to the approximate diameter of one catalyst bead, forming a single layer.
- **Reactor Volume**: The volume (V) of the reactor where the reaction took place was calculated using the formula (1). With a radius (r) of 0.6475 cm and a catalyst bed height (h) of 0.1 cm, the volume was determined to be: V=0.1319cm^3
- **Gas Hourly Space Velocity (GHSV)**: The GHSV was set at 20,509 h^{-1}. The flow rate (Q) was 45 ml/min. The GHSV was calculated using the formula (2) GHSV=20,509h^{-1}
- **Oven Type**: The oven used was a Nabertherm RT 50/250/11 with a P330 controller.
- **Temperature Program**: The oven temperature was increased by 50°C every 10 minutes and held at the reached temperature for another 30 minutes, resulting in a total duration of 40 minutes at each temperature. Measurements were taken at the following temperatures: 20°C (initial), 100°C, 150°C, 200°C, 250°C, 300°C, 350°C, 400°C, 500°C.

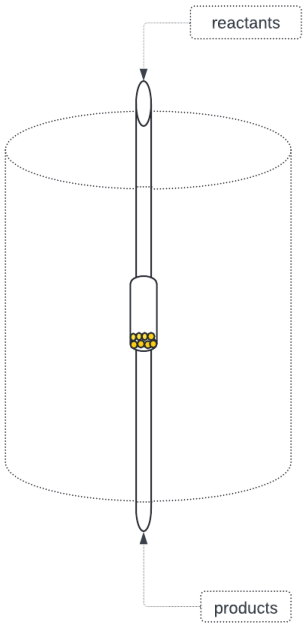

Figure 14: Oven reactor

3.2.5. Instruments

- **Plasma Generation**: The DBD plasma was generated using a JOY-IT DPS instrument.
- **Gas Chromatograph**: The outlet gases from the reactor were analyzed using a BRUKER SCION 436 GC gas chromatograph equipped with a Thermal Conductivity Detector (TCD) and a PORAPAC - Q column. Helium was used as the carrier gas.
    - **Operation**: The sample gases were introduced into the gas chromatograph where they were driven into the column by helium. Within the column, the sample components were separated, and their presence was indicated by signal generation. The signals were transmitted to a computer using the Compass CDS network chromatography system software.

3.2.6. Gas Flow Measurement

- **Flow Rates**: Gas flow rates were determined by the computer's get red-y program and provided by the corresponding mechanical equipment via red-y measures from Vögtlin.

3.2.7. Catalyst Preparation

Each catalyst (CeO_2, CeO_2/CuO 10%, and CeO_2/CuO 20%) was prepared according to standard procedures and characterized for surface area and pore size.

Preparation of the beads
The beads have been prepared by modifying the method reported Chalkia et al. [69] by introducing high-power ultrasounds and an automated syringe pump. A mixture of 5wt% Polyethersulfone (PESf) Ultrason E6020P (provided by BASF SE, Germany) with 1wt% polyvinylpyrrolidone (PVP) K30 (purchased from Alfa Aesar, Germany), is dissolved in 4,85 ml N-methyl-2-pyrrolidone (NMP) , Merck KGaA. 44 wt% CeO_2 was added to this mixture resulting to a slurry with 50wt% solid content. This slurry was sonicated for 15 minutes at 26,4 W/cm^2. The sonication leads to a deagglomeration of the ceria powder and also to degassing of the slurry.

The additional decoration of the ceria beads with metallic Copper particles was prepared by adding to the slurry 10 and 20 % metal based on the ceria content. Specifically, particles with a particle size distribution of 0,75 – 1,5 μm were used.

The sonicated slurry was then dropped to a big beaker with distilled water with 0,1 ml/min using an automated syringe pump. The needle has had a diameter of 1.7 mm.
The distance between the needle and water surface was 20 mm. The beads are left in the water for 24 h in order to let the phase inversion (coagulation and solvent exchange) to take place.

The beads with and without metal addition have been heated up to 1300 °C with 2 K/min (with an intermediate step for 1 h at 300 °C) and sintered at 1300 °C for 5 h.

In Figure 15 SEM micrographs of the three bead series (pure Ceria and with Cu) are presented

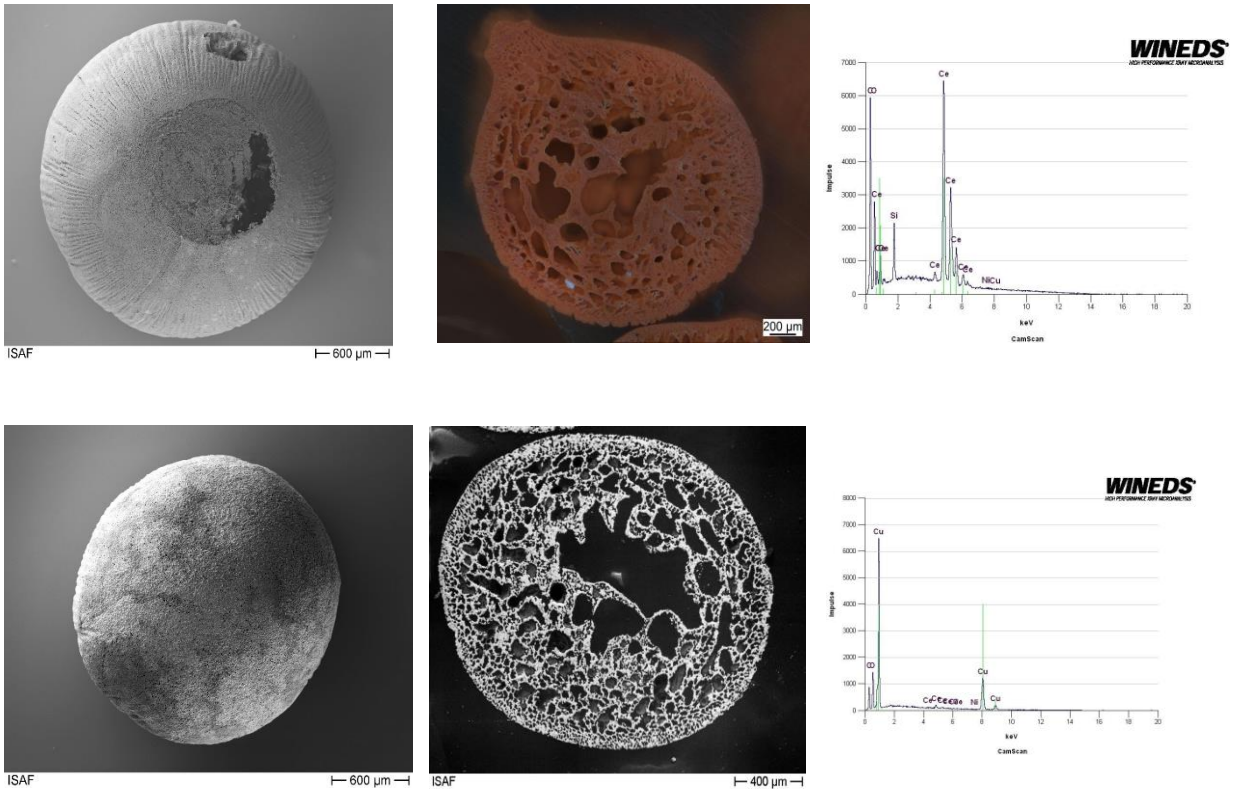

Figure 15: Optical microscope and SEM/EDS pictures of Ceria beads (top) and Copper doped ceria (bottom).

3.2.8. Procedure

The following table exhibits the conditions in which the experiments took place

Table 1: The table consists of the source of energy, the mass of the catalyst, the GHSV, the Voltage/Temperature and the Sampling time of each experiment.

Experiment	**Method**	**Catalyst**	**Catalyst Mass (g)**	**GHSV (h^{-1})**	**Voltage/ Temperature**	**Sampling time (min)**
1	Thermal	CeO_2	0.1589	20.509	20,100,150,200, 250, 300,350, 400, 500°C	1, 31, 61, 91, 121,151,181,201,231
2	Thermal	CeO_2/CuO 10%	0.2626	20.509	20,100,150,200, 250, 300,350, 400, 500°C	1, 31, 61, 91, 121,151,181,201,231
3	Thermal	CeO_2/CuO 20%	0.2428	20.509	20,100,150,200, 250, 300,350, 400, 500 °C	1, 31, 61, 91, 121,151,181,201,231
4	Plasma	None	0	20,352	5, 7, 10 kV	3, 13, 23
5	Plasma	CeO_2	0.3965	20,352	5, 7, 10 kV	3, 13, 23
6	Plasma	CeO_2/CuO 10%	0.3987	20,352	5, 7, 10 kV	3, 13, 23
7	Plasma	CeO_2/CuO 20%	0.3925	20,352	5, 7, 10 kV	3, 13, 23
8	Plasma	CeO_2/Cu (reduced) 20%	0.3865	20,352	10 kV	3, 13, 23, 33, 43, 53, 63, 73, 83

The following is a standard procedure of experiments:

1. Reactor Loading: The catalyst was loaded into the reactor, ensuring a uniform single layer with a bed height of 0.1 cm. The exact masses of catalysts used were:

- **Blank Experiment**: No catalyst
- **CeO_2**: 0.3965 g for plasma, 0.1589 g for oven
- **CeO_2/CuO 10%**: 0.3987 g for plasma, 0.2626 g for oven
- **CeO_2/CuO 20%**: 0.3925 g for plasma, 0.2428 g for oven
- **CeO_2/Cu 20%(reduced):** 0.3865 g only for plasma

2.Reaction Conditions: The gas feed was introduced and after stabilization the reactor was brought to the desired temperature using either DBD plasma or an oven

3.Thermal (Oven) Experiments: The oven temperature was increased by 50°C every 10 minutes and held at each temperature for 30 minutes. Measurements were taken at the following temperatures: 20°C, 100°C, 150°C, 200°C, 250°C, 300°C, 350°C, 400°C and 500°C. Each measurement was taken at the midpoint of the hold time (i.e., after 20 minutes of total time at each temperature).

The sampling process was as follows:

- **Sample Collection**: The first sample was assumed to occur at 3 minutes to allow 2 minutes for the plasma to interact with the reactants and 1 minute for the chromatograph to collect the sample. Subsequent samples were taken at 10-minute intervals.
- **Chromatograph Analysis**: Each sample required 1 minute for collection and 9 minutes for analysis, resulting in a total cycle time of 10 minutes per sample.

4.Plasma Experiments: Each plasma experiment was conducted at three different voltages: 5 kV, 7 kV, and 10 kV. Samples were taken at each voltage at 3 minutes, 13 minutes, and 23 minutes.

5.Data Collection: Reaction products were analyzed using gas chromatography, and conversion rates of CO_2 to hydrocarbons and other products were recorded. The areas of the chromatographs corresponded to the concentration of reactants and products.

3.2.9. Data Analysis

The performance of the catalysts under different energy sources was compared by analyzing the conversion efficiency, selectivity, and yield of the desired products. The areas of the chromatographs were used to determine the concentrations of reactants and products, providing a basis for evaluating the effectiveness of the catalytic processes. Statistical analysis was performed to assess the significance of the differences observed.

This structured approach provides a clear and comprehensive overview of the materials and methods used in the study, facilitating reproducibility and understanding of the experimental procedures.

3.2.10. Calculations

In this chapter, we detail the key calculations and equations used to analyze the performance of the catalysts in the CO_2 hydrogenation experiments. These include equations for selectivity, yield, CO_2 conversion, and CO_2 reaction rate.

The CO_2 conversion (X_{CO2}) measures the fraction of CO_2 that is converted into products. It is calculated using the following equation:

$$X_{CO2}(\%) = \frac{C_{CO2,in} - C_{CO2,out}}{C_{CO2,in}} \times 100 \quad (3)$$

Where:

- $C_{CO2,in}$ is the concentration of CO_2 at the reactor inlet.
- $C_{CO2,out}$ is the concentration of CO_2 at the reactor outlet.

Selectivity (S) indicates the preference of the catalyst for producing a specific product from CO2. It is calculated as:

$$S_{CO} = \frac{C_{CO}}{C_{CO} + C_{CH4}} \times 100 \quad (4)$$

$$S_{CH4} = \frac{C_{CH4}}{C_{CO} + C_{CH4}} \times 100 \quad (5)$$

Where:

- C_{CO} is the concentration of CO
- $C_{CH4}$is the concentration of CH_4

Yield (Y) of a product provides the amount of that product formed per unit amount of CO_2 fed into the reactor. It is calculated as:

$$Y_{CO} = \frac{S_{CO} \times X_{CO2}}{100} \quad (6)$$

$$Y_{CH4} = \frac{S_{CH4} \times X_{CO2}}{100} \quad (7)$$

The CO_2 reaction rate (r) quantifies the amount of CO_2 converted per unit time per unit mass of catalyst. It is typically expressed in (mol s^{-1} g^{-1})

$$r = \frac{X_{CO2} \times C_{CO2,in} \times F}{m_{cat} \times V_m \times 60 \times 10^6} \quad (8)$$

Where:

- F is the molar flow rate of CO_2 at the reactor inlet.
- m_{cat} is the catalyst's mass
- V_m is the gas constant
- $C_{CO2,in}$ is the initial CO_2 concentration expressed in ppm.

4. Results

4.1. Hydrogenation of Carbon Dioxide with the Thermal Method

4.1.1. Cerium Oxide (CeO_2)

Figure 16 illustrates the relationship between the conversion (%) of CO_2 and temperature using CeO_2 as catalyst and heat as a source of energy. The temperatures range from 200°C to 500°C and the conversion from 0% to 22%.

As shown in Figure 16 the hydrogenation reaction does not take place until 500 °C. Between 200-500 °C the CO_2 conversion is almost 0%, it fluctuates between 0-2%. At 500 °C the CO_2 conversion increases to 22%. This could possibly suggest that the activity of CeO_2 is limited at temperatures 20-500 °C and that a higher activation energy is required for the reaction with CeO_2 as catalyst.

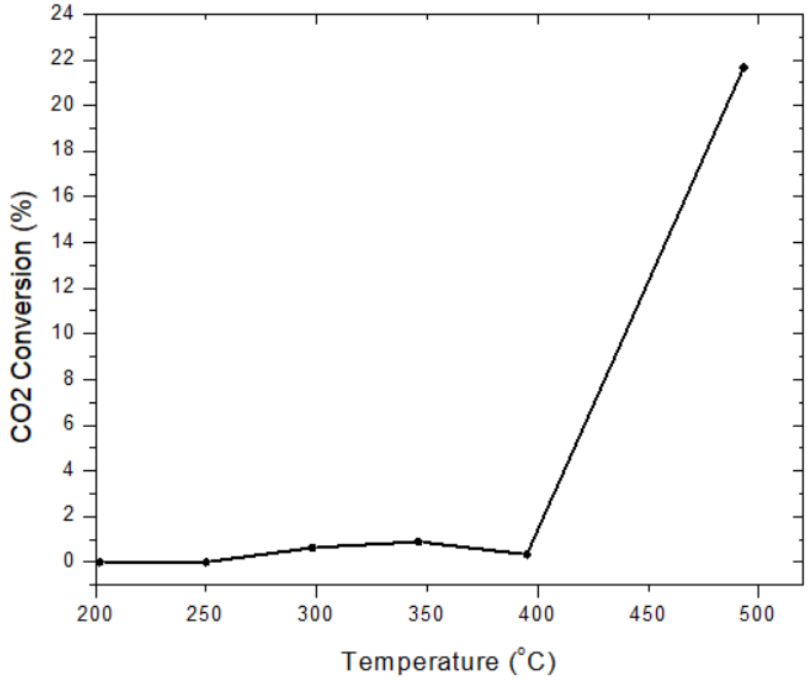

Figure 16: Relationship between CO_2 Conversion (%) and Temperature (°C) with CeO_2

As mentioned before, at temperatures below 500°C the activity of CeO_2 0%. However, at 500°C there is an increase in catalyst's activity. Hence, higher temperatures are required to achieve CO_2 conversion with this catalyst.

For practical applications, this suggests that CeO_2 can be an effective catalyst for CO_2 hydrogenation at high temperatures, and further optimization might help to lower the activation temperature while maintaining high conversion efficiency.

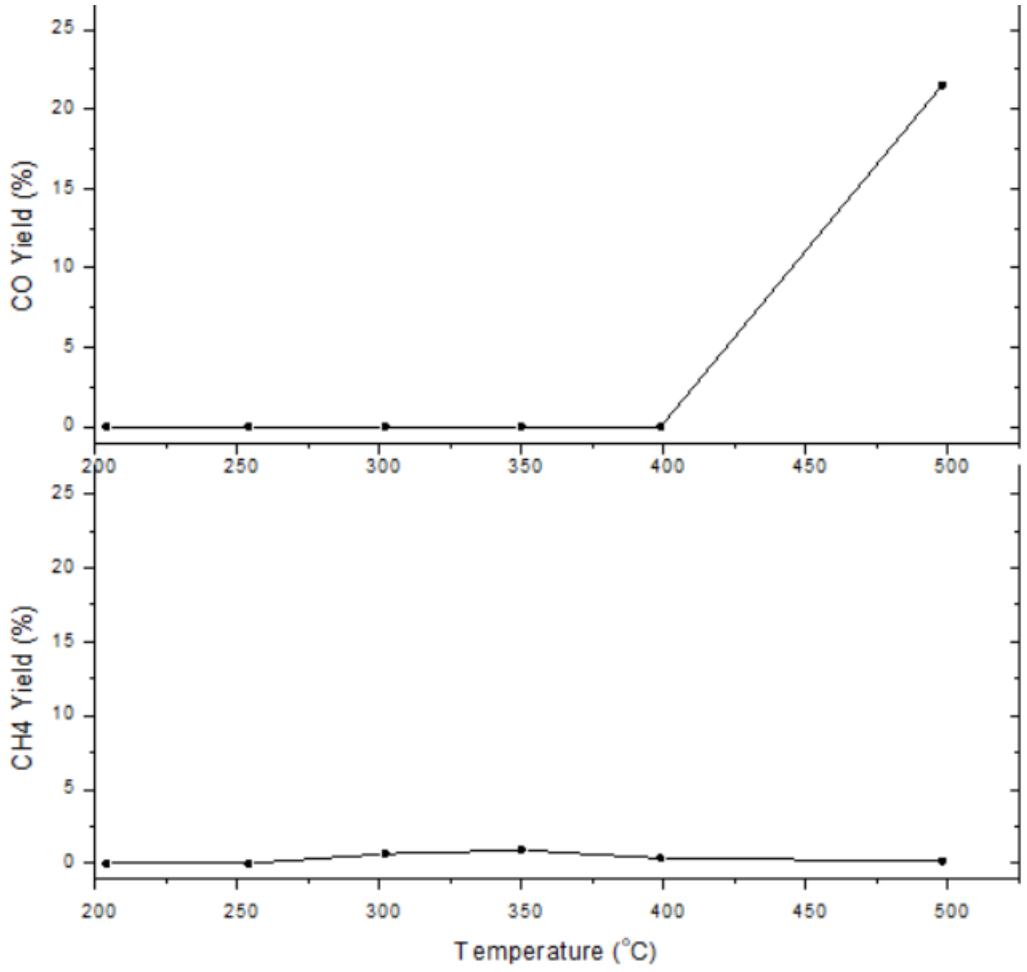

Figure 17: Relationship between CO, CH_4 yield (%) and Temperature (^oC) with CeO_2

The products of the hydrogenation reaction as discussed in Section 2 are carbon monoxide (CO), methane (CH_4) and methanol (CH_3OH). However, using CeO_2 as a

catalyst gave only CO and CH_4. Figure 17 illustrates the relationship between yields of CO and CH_4 (%) and temperature (°C).

The temperature range is between 200-500 °C. As mentioned in Figure 16 the reaction starts to occur at 500 °C. This statement applies for the products as well. At temperatures from 200°C to 400°C, the CO yield is 0%. This could mean that CeO_2 has limited activity in producing CO through CO_2 hydrogenation in the low to mid-temperature range under the thermal conditions. CO starts to form at 500 °C where the CO yield reaches approximately 22%.

On the other hand, CH_4 yield seems to be very low throughout the whole temperature range. At 300-400 °C there is a slight production of methane, approximately 1-2%. This indicates that the formation of CH_4 is not favored on the CeO_2 catalyst under these conditions.

According to Figures 16 and 17, CeO_2 shows a significant activity at high temperatures (over 500 °C). The low yield at temperatures below 400 °C means that the energy delivered to the system is inefficient to exceed the activation energy of the hydrogenation reaction. Furthermore, the catalyst is selective towards CO.

CH_4 yields are very low with CeO_2, suggesting that ceria is not effective for methane formation. This could be due to the lack of sufficient active sites for methanation or unfavorable reaction pathways on the CeO_2 surface.

For practical applications, the results suggest that while CeO_2 can be an effective catalyst for CO production for CO_2 hydrogenation at high temperatures, it is not suitable for methane production under the conditions tested. Further optimization or alternative catalysts may be needed to achieve higher CH_4 yields.

4.1.2. Cerium Oxide/ Copper Oxide (CeO_2/CuO 10%)

Figure 18 illustrates the relationship between the conversion (%) of CO_2 and temperature using CeO_2/CuO 10% as catalyst and heat as a source of energy. The temperatures range from 200°C to 500°C and the CO_2 conversion from 0% to 24%.

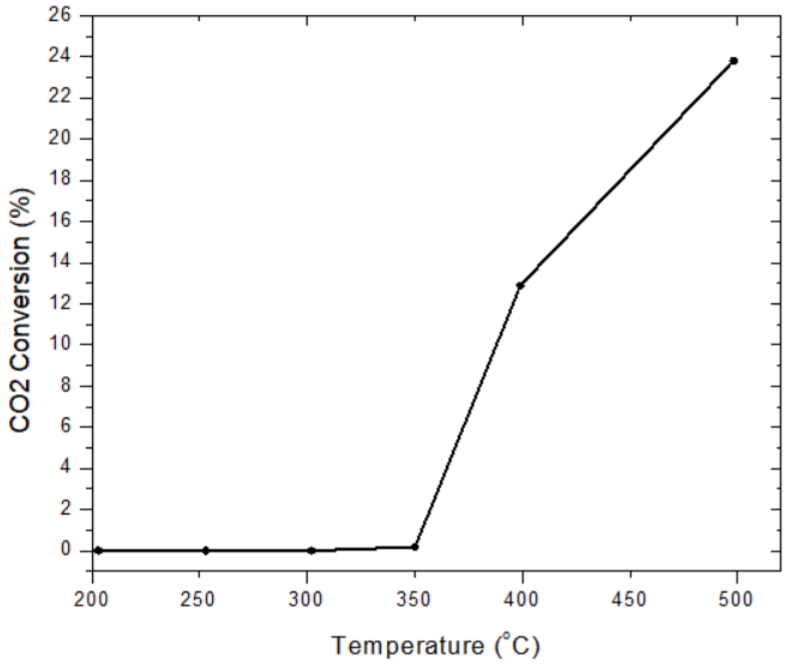

Figure 18: Relationship between CO_2 Conversion (%) and Temperature (°C) with CeO_2/CuO 10%

As shown in Figure 18 the hydrogenation reaction does not take place until 400 °C. Between 200-400 °C the CO_2 conversion is almost 0%, it fluctuates between 0-2%. At 400°C the CO_2 conversion increases to 12-14%. A significant increase in CO_2 conversion is observed at 500°C, where the conversion rate sharply rises to approximately 24%. This indicates that the activity of CeO_2/CuO 10% is limited at temperatures 20-400 °C and that a higher activation energy is required for the reaction with CeO_2/CuO 10% as catalyst.

As mentioned before, at temperatures below 350°C the activity of CeO_2/CuO 10% is low. However, at 400°C there is an increase in catalyst's activity and further at 500°C. Hence, higher temperatures are required to achieve CO_2 conversion with this catalyst. The gradual increase in conversion starting at 400°C suggests that the addition of CuO to CeO_2 lowers the activation energy of the hydrogenation reaction compared to pure CeO_2, enhancing the catalyst's performance.

For practical applications, this suggests that CeO_2/CuO 10% can be an effective catalyst for CO_2 hydrogenation at high temperatures, and further optimization might help to lower the activation temperature while maintaining high conversion efficiency.

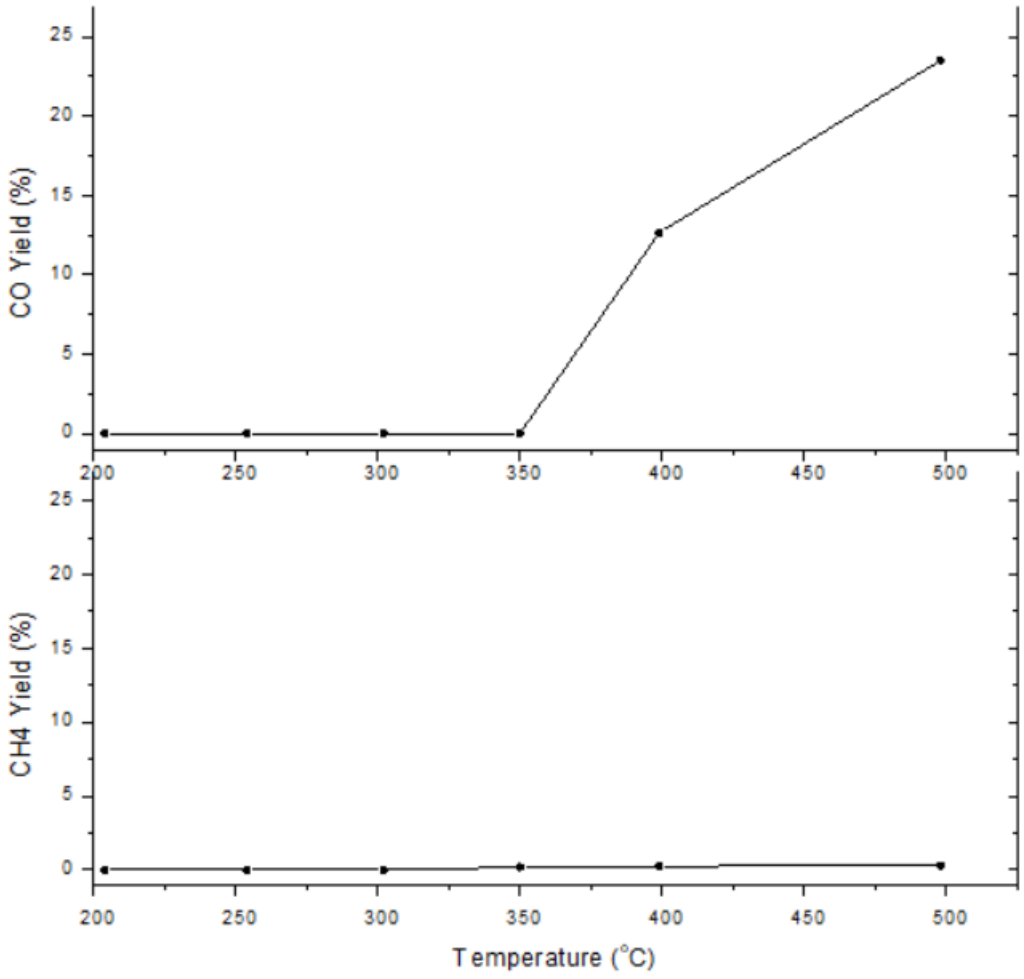

Figure 19: Relationship between CH_4, CO yield (%) and Temperature (^{0}C) with CeO_2/CuO 10%

Once again, using CeO_2/CuO 10% as a catalyst gave only CO and CH_4. Figure 19 illustrates the relationship between yields of CO and CH_4 (%) and temperature (°C).

The temperature range is between 200-500 °C. As mentioned in Figure 18 the reaction starts to occur at 400 °C. This statement applies for the products as well. At temperatures from 200°C to 350°C, the CO yield is 0%. This could mean that CeO_2/CuO 10% has limited activity in producing CO through CO_2 hydrogenation in the low to mid-temperature

range under the thermal conditions. CO starts to form at 400 °C where the CO yield is 14% and at 500 °C approximately 23%.

On the other hand, CH_4 yield seems to be very low, close to 0%,throughout the whole temperature range.

For practical applications, the results suggest that while CeO_2/CuO 10% can be an effective catalyst for CO production from CO_2 hydrogenation at high temperatures, it is not suitable for methane production under the conditions tested. Further optimization or alternative catalysts may be needed to achieve higher CH_4 yields.

4.1.3. Cerium Oxide/ Copper Oxide (CeO_2/ CuO 20%)

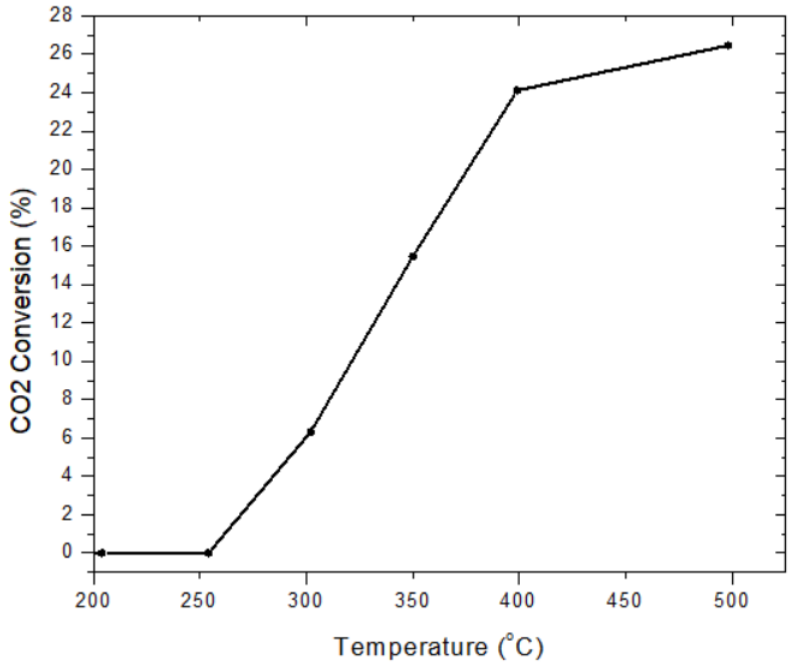

Figure 20: Relationship between CO_2 Conversion (%) and Temperature (°C) with CeO_2/CuO 20%

Figure 20 depicts the relationship between the conversion (%) of CO_2 and temperature using CeO_2/CuO 20% as a catalyst and heat as a source of energy. The temperatures range from 200°C to 500°C, and the corresponding CO_2 conversion percentages are plotted.

As shown in Figure 20 the hydrogenation reaction does not take place until 250 °C. Between 200-250 °C the CO_2 conversion is almost 0%, it fluctuates between 0-2%. At 300°C

the CO_2 conversion increases to 5-6%. A significant increase in CO_2 conversion is observed at 350°C, where the conversion rate sharply rises to approximately 16% and finally at 500°C the conversion reaches 26%. This indicates that the activity of CeO_2/CuO 20% is limited until 250 °C. So far CeO_2/CuO 20% is the best performing catalyst.

Concluding, at temperatures below 250°C the activity of CeO_2/CuO 20% is low. However, at 300°C there is an increase in catalyst's activity. Hence, higher temperatures are required to achieve CO_2 conversion with this catalyst. The gradual increase in conversion starting at 300°C suggests that the addition of CuO to CeO_2 lowers the activation energy of the hydrogenation reaction compared to pure CeO_2, enhancing the catalyst's performance.

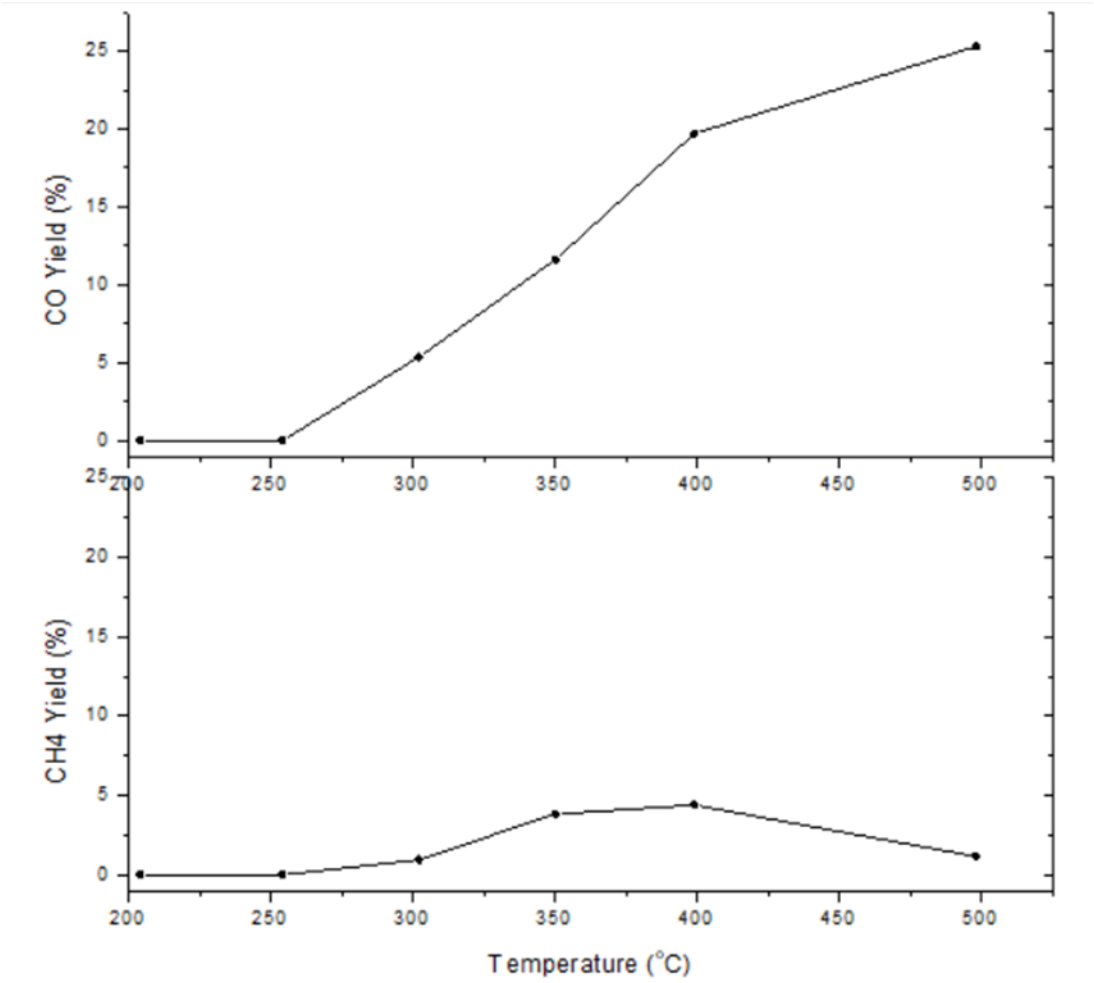

Figure 21: Relationship between CO, CH_4 yield (%), and Temperature (°C) using a CeO_2/CuO 20% catalyst.

Figure 21 illustrates the CH_4 and CO yields (%) plotted with temperature (°C). Once again, it is noticeable that the catalyst CeO_2/CuO 20% has a high selectivity to CO. The temperatures range from 200°C to 500°C, and the corresponding yields for CO and CH_4 are plotted.

The CeO_2/CuO 20% catalyst's low activity at temperatures below 300°C suggests that higher energy input is necessary to activate the catalyst effectively. Higher temperatures (300-500°C) are required to convert CO_2 to CO.

Methane yield seems again to be low (close to 5% at 350-400 °C). This low yield of CH_4 suggests that CeO_2/CuO 20% is not an effective catalyst for methane formation under

these conditions. This could be due to the lack of sufficient active sites for methanation or unfavorable reaction pathways on the CeO_2/CuO 20% surface.

For practical applications, the results suggest that while CeO_2/CuO 20% can be an effective catalyst for CO production from CO_2 hydrogenation at high temperatures, it is not suitable for methane production under the conditions tested. Further optimization or alternative catalysts may be needed to achieve higher CH_4 yields.

4.1.4. CO_2 Conversion and Selectivity Comparison Diagrams

In this section, the results that were discussed in previous sections are compared. Figure 22 illustrates the CO_2 conversion percentages as a function of temperature using three different catalysts: CeO_2, CeO_2/CuO 10%, and CeO_2/CuO 20%. The temperatures range from 200°C to 500°C, and the corresponding CO_2 conversion percentages are plotted for each catalyst.

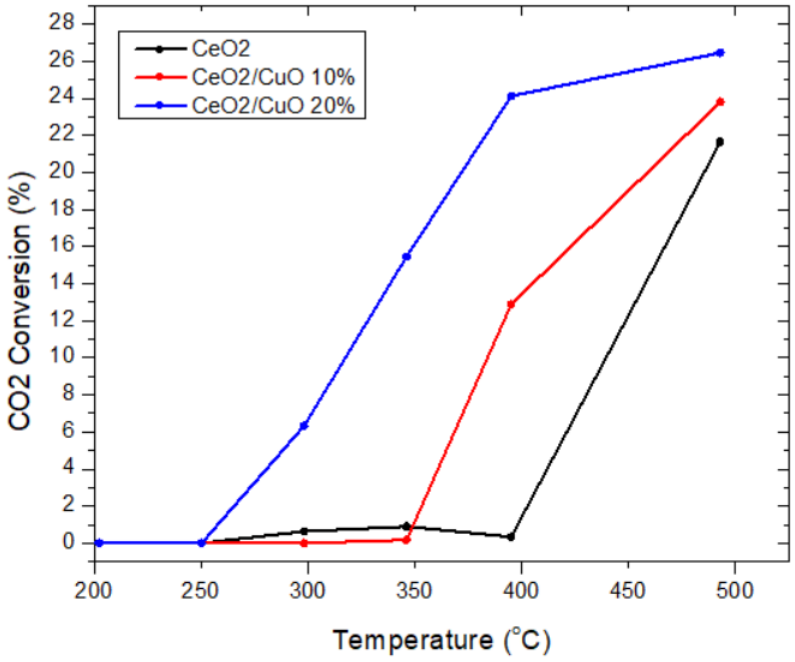

Figure 22: Performance comparison of the three catalysts.

As depicted in Figure 22, all three catalysts' CO_2 conversion is temperature-dependent. Specifically, the hydrogenation reduction reaction with CeO_2 starts at 500 °C and a 22%

conversion is achieved. For CeO_2/CuO 10%, the reaction starts to occur at 400 °C and for CeO_2/CuO 20% at 300 °C. This indicates that the loading of CuO enhances the catalysts' performance. The greater the CuO loading, the better the catalysts' performance in this case.

The addition of CuO to CeO_2 lowers the activation temperature required for CO_2 conversion, as seen with both CeO_2/CuO 10% and CeO_2/CuO 20% showing significant activity at lower temperatures compared to pure CeO_2. Higher CuO content (20%) further improves the catalyst's activity, achieving the highest conversion rates and an earlier onset of activity.

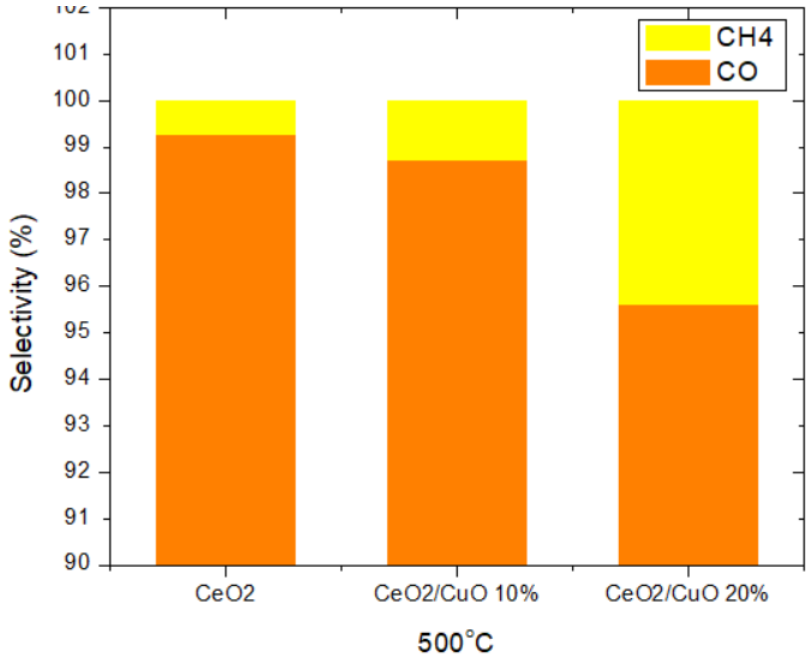

Figure 23: Products' selectivity at 500°C.

According to Figure 23, all three catalysts (CeO_2, CeO_2/CuO 10%, and CeO_2/CuO 20%) exhibit very high selectivity towards CO at 500°C. In conclusion, the primary product of CO_2 hydrogenation is CO across all catalysts. Specifically, CeO_2 is 99% CO-selective, CeO_2/CuO 10% is 98% CO-selective and CeO_2/CuO 20% 96% CO- selective. The selectivity towards CH_4 is consistently low for all three catalysts, with only marginal differences observed among them. This suggests that these catalysts are not effective for methane formation under the conditions tested.

4.2. Hydrogenation of Carbon Dioxide with plasma

4.2.1. No catalyst

Figure 24 illustrates the power (kW) as a function of time for plasma. As it is visible the power is constant.

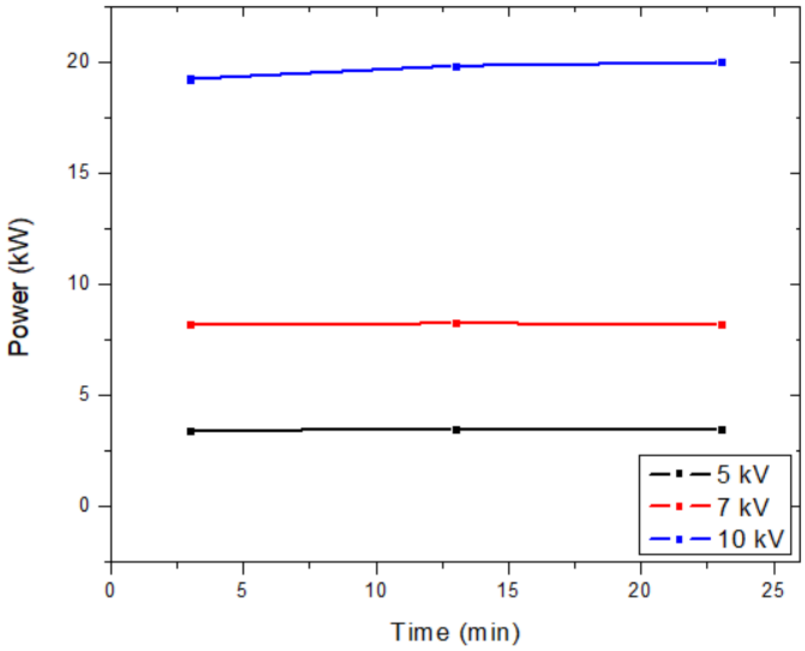

Figure 24: Relationship between Power (kW) and time (min)

Figure 25 shows the CO_2 conversion (%) as a function of time for the plasma method without a catalyst. The experiments were conducted at three different voltages: 5 kV, 7 kV, and 10kV, with measurements taken at 3 minutes, 13 minutes, and 23 minutes. At 5 kV, the conversion is minimal and remains steady around 2-3%. At 7 kV, the conversion is moderate, staying around 8-10%. At 10 kV, the conversion is significantly higher, starting at 14% and increasing slightly to 16% over time. The CO_2 conversion remains

relatively steady for 5 kV and 7 kV. This suggests that the applied voltage plays a more critical role in determining the CO_2 conversion rate than the time without a catalyst. Without a catalyst, the plasma method still achieves some degree of CO_2 conversion, primarily influenced by the applied voltage but the conversion is minimal.

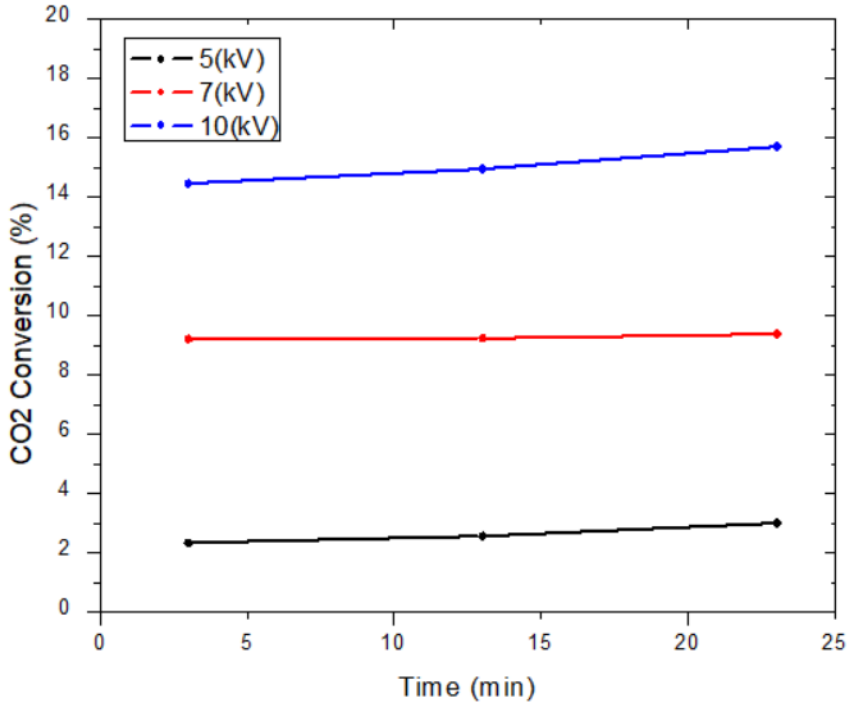

Figure 25: CO_2 conversion at 5, 7 and 10 kV.

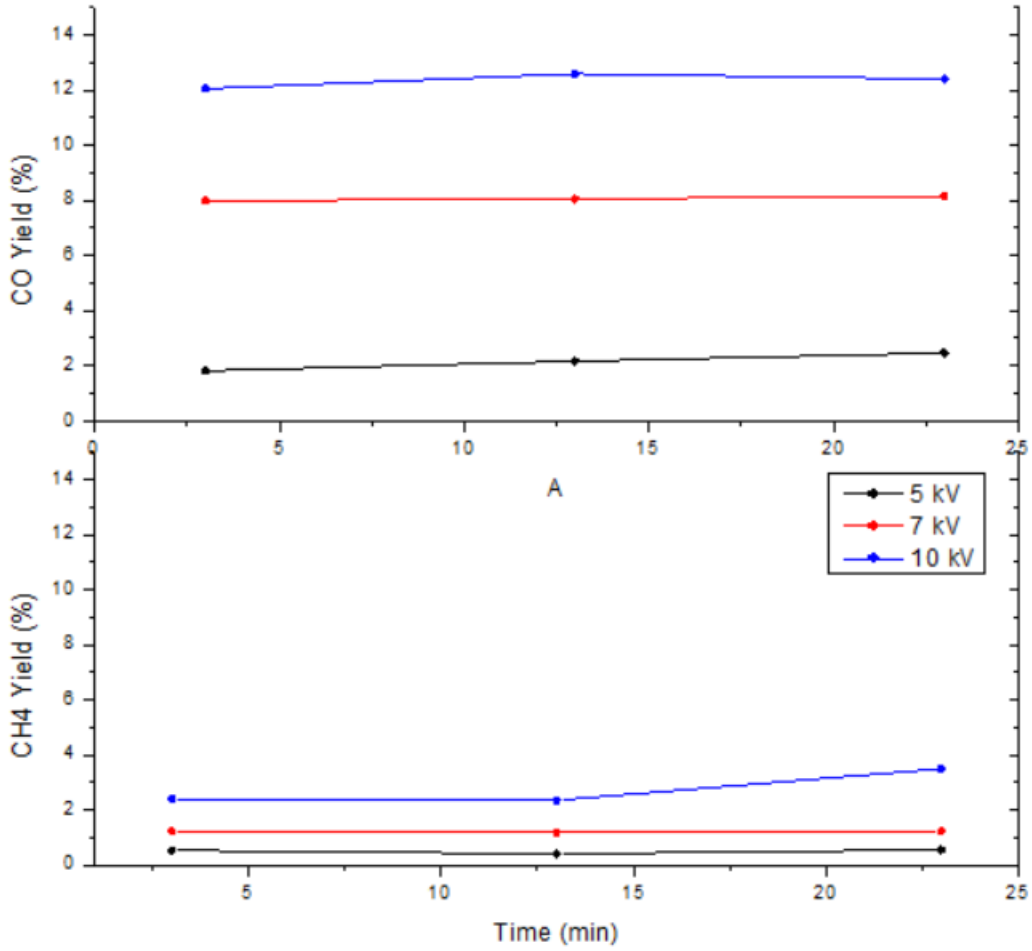

Figure 26: Relationship between CO, CH_4 yield (%) and time (min) with no catalyst.

Figure 26 displays the yield percentages of CO and CH_4 over time for the plasma method without a catalyst, with experiments conducted at voltages of 5 kV, 7 kV, and 10 kV. Measurements were taken at 3 minutes, 13 minutes, and 23 minutes. At 5 kV, the CO yield is approximately 2% and the CH_4 yield is 0.5%. At 7 kV, the CO yield is 8% and the CH_4 yield is about 1%. At 10 kV, the CO yield reaches 12% and the CH4 yield is 2%. The measurements remain stable over time across all voltages. The plasma method, even without a catalyst, effectively converts CO_2 to CO and CH_4, with CO being the dominant product. Higher voltages enhance the plasma energy, leading to increased CO_2 conversion rates and higher yields of CO and CH_4.

4.2.2. Cerium Oxide (CeO_2)

Figure 27 represents the CO_2 conversion (%) as a function of time using CeO_2 as the catalyst. The experiments were taken at 5, 7 and 10 kV at 3, 13 and 23 minutes. At 5 kV the CO_2 conversion is at approximately 7%, at 7 kV at 14% and at 10 kV is reaching 23%. The CO_2 conversion rate increases with higher applied voltages. The highest conversion rate is observed at 10 kV, followed by 7 kV and 5 kV. For all three voltages, the CO_2 conversion remains relatively stable over the 23-minute period, indicating that the reaction reaches a steady state quickly and maintains consistent conversion rates.

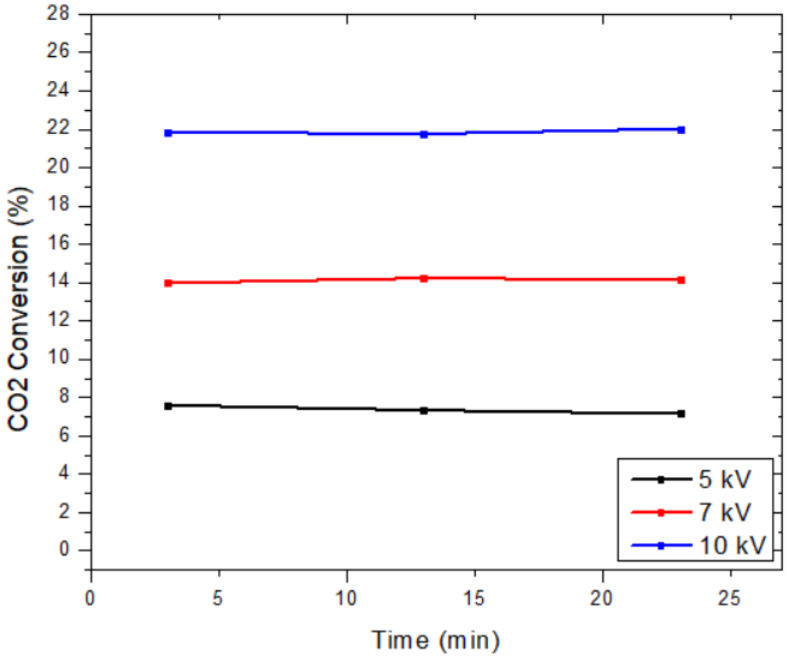

Figure 27: CO_2 conversion overtime at 5, 7 and 10 kV with CeO_2 catalyst.

The CO_2 conversion remains steady for all three voltages, indicating that the reaction stabilizes quickly and maintains a consistent conversion rate throughout the experiment. The presence of the CeO_2 catalyst helps to stabilize the plasma, leading to more consistent CO_2 conversion rates over time.[70],[71] Catalysts can provide additional surfaces for the reactions to occur, which can help to distribute the energy more evenly and reduce fluctuations in the plasma. [72]

The CeO_2 catalyst can help to moderate the localized temperature increases that occur at higher voltages, leading to more stable reaction conditions. This can prevent the large

temperature fluctuations that might otherwise cause instability in the conversion rates. [73]

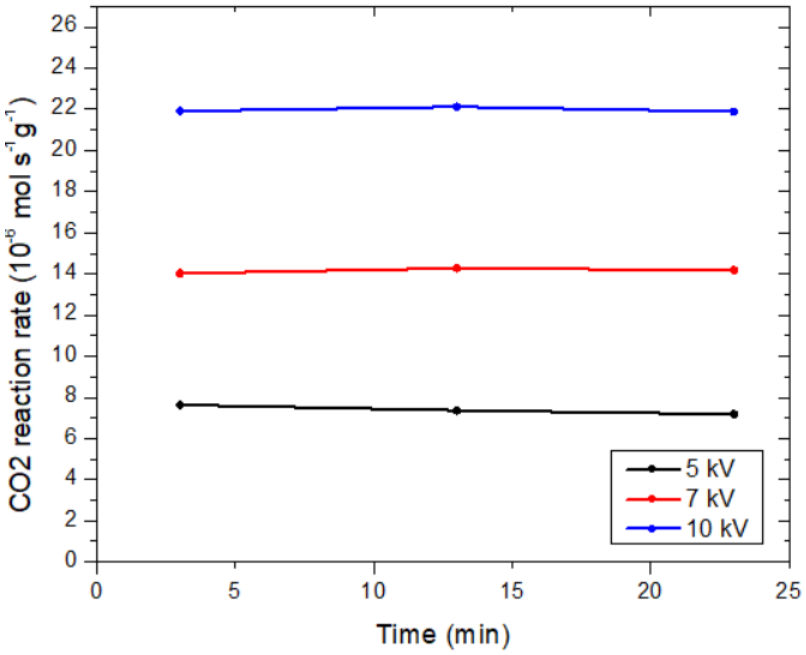

Figure 28: CO_2 reaction rate at 5,7 and 10 kV with CeO_2 catalyst.

Figure 28 depicts the CO_2 reaction rate (10^{-6}mol $s^{-1}g^{-1}$) as a function of time for the plasma method using CeO_2 as the catalyst. The experiments were at 5, 7 and 10 kV at 3 minutes, 13 minutes, and 23 minutes. At 5 kV the CO_2 reaction rate is approximately 7x10^{-6}mol $s^{-1}g^{-1}$, at 7 kV the reaction rate is 14x10^{-6}mol $s^{-1}g^{-1}$ and at 10 kV 22x10^{-6}mol $s^{-1}g^{-1}$. The reaction rate at all 3 voltages remains stable.

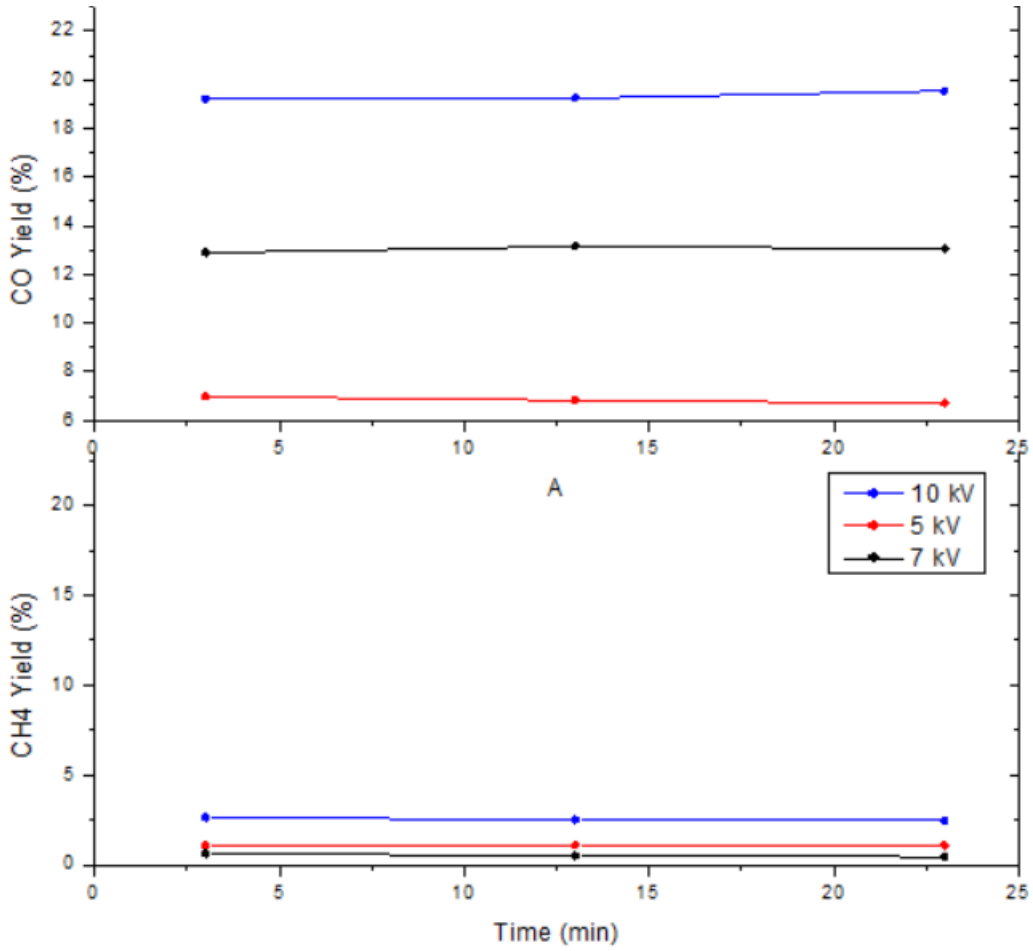

Figure 29: Relationship between CO, CH_4 yield (%) and Temperature (^oC) using a CeO_2 catalyst.

Figure 29 illustrates the yield percentages of CO and CH_4 over time for the plasma method using CeO_2 as a catalyst. The experiments were carried out at voltages of 5 kV, 7 kV, and 10 kV, with data collected at 3, 13, and 23 minutes. At 5 kV, the CO yield is around 8%, and the CH_4 yield is approximately 0.5%. At 7 kV, the CO yield is about 14%, with a CH_4 yield of roughly 2%. At 10 kV, the CO yield reaches 20%, and the CH_4 yield is around 5%. The yields remain stable throughout the experiments.

4.2.3. Cerium oxide doped with 10% copper oxide (CeO_2/CuO 10%)

Figure 30 depicts the CO_2 conversion (%) as a function of time using CeO_2/CuO 10% as the catalyst.

.

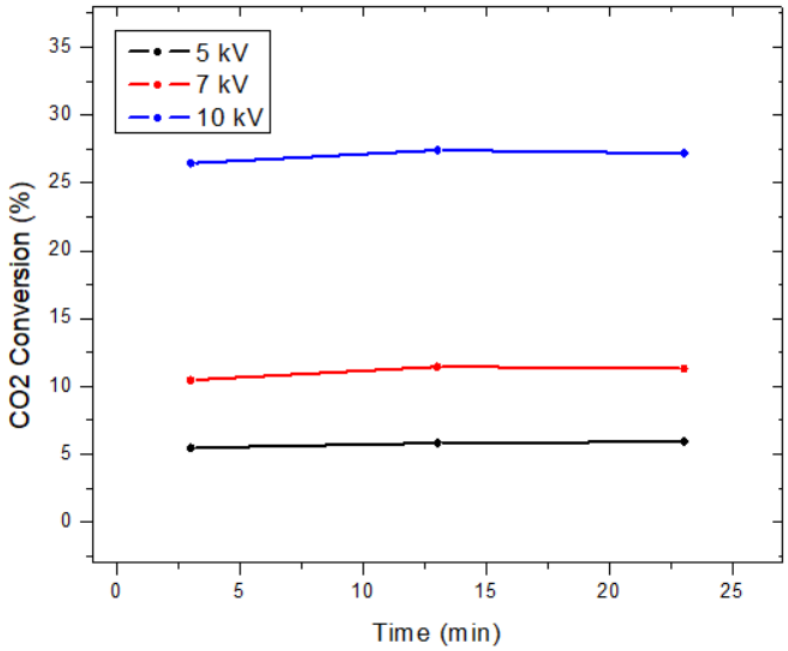

Figure 30: CO_2 conversion at 5, 7, 10 kV with CeO_2/CuO 10% catalyst.

The CO_2 conversion over time is relatively stable in all three voltages. At 5 kV the CO_2 conversion is at 5%, at 7 kV 11% and at 10 kV 26%. The catalyst provides active sites that facilitate the conversion of CO_2. At higher voltages, the energy delivered to the system is increased and so are the reactive species (e.g. radicals, ions) that interact with the catalyst surface. This results in a more stable and efficient conversion. Also, the catalyst can absorb and distribute heat more evenly within the reactor, preventing hot spots and ensuring a more uniform temperature profile. This can lead to more stable reaction rates as the operating conditions remain consistent.

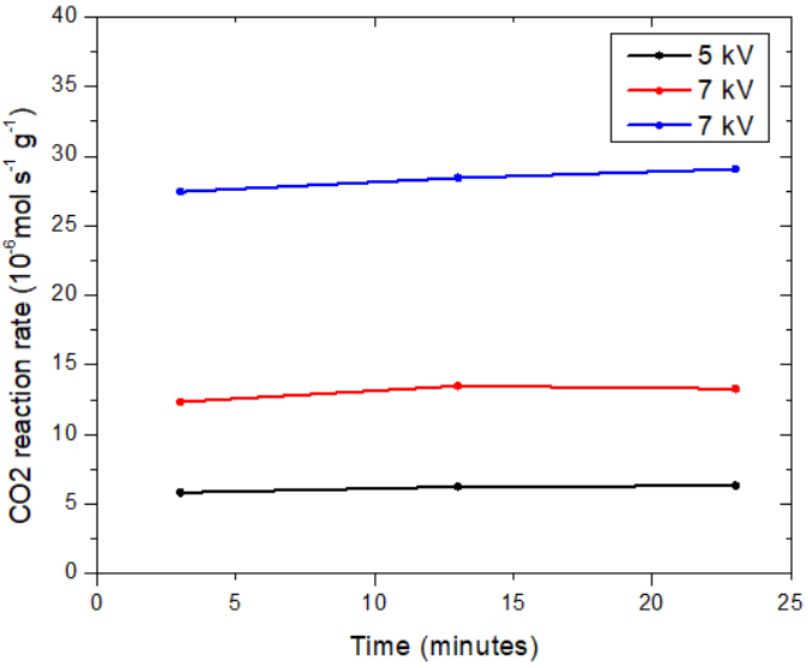

Figure 31: CO_2 reaction rate at 5, 7 and 10 kV

Figure 31 shows the CO_2 reaction rate (10^{-6}mol $s^{-1}g^{-1}$) as a function of time (minutes) using CeO_2/CuO 10%. The experiments were conducted at 5,7 and 10 kV and the measurements were taken at 3,13 and 23 minutes.

At 5 kV the CO_2 reaction rate is 7x10^{-6}mol $s^{-1}g^{-1}$, at 7 kV 13x10^{-6}mol $s^{-1}g^{-1}$ and at 10 kV it fluctuates between 26-27x10^{-6}mol $s^{-1}g^{-1}$. The CO_2 reaction rate increases with higher applied voltages. Generally, for all three voltages, the CO_2 reaction rate remains steady over the 23 minutes, indicating that the reaction stabilizes quickly and maintains a consistent rate throughout the experiment.

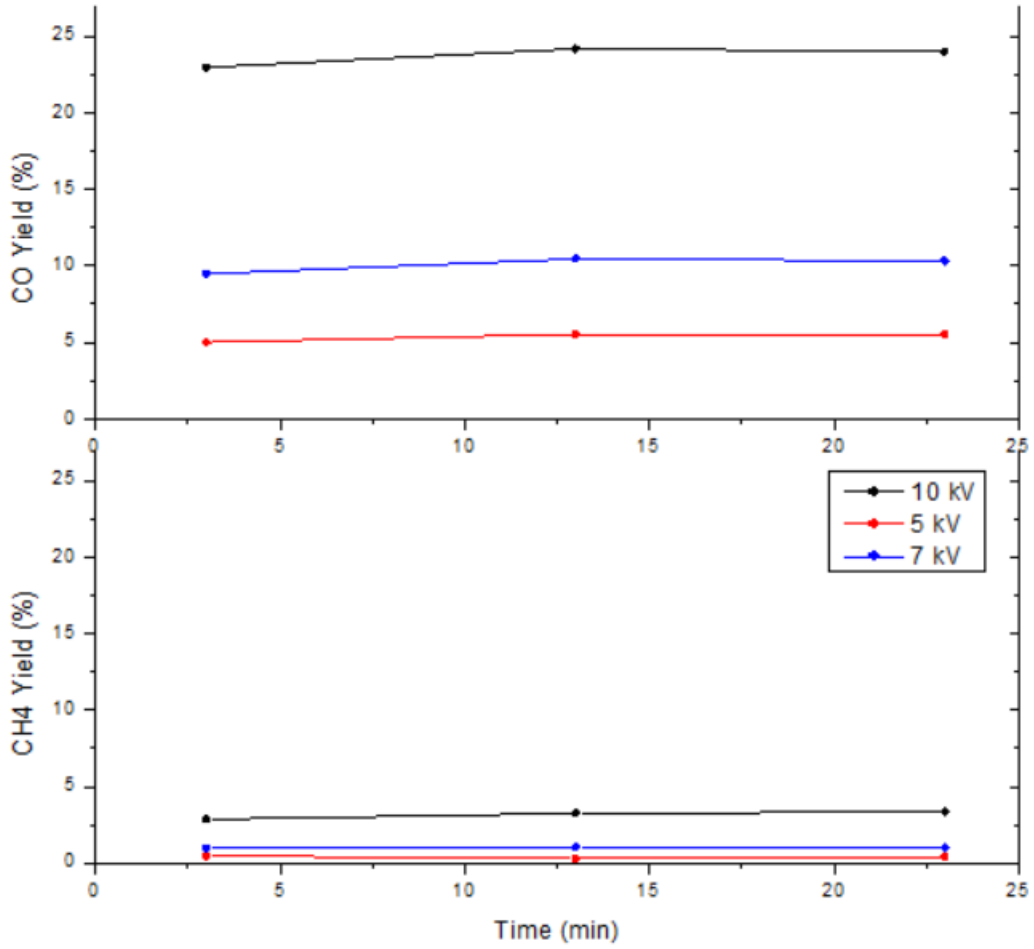

Figure 32: Relationship between CO, CH_4 yield (%) and Temperature (^oC) using a CeO_2/CuO 10% catalyst.

Figure 32 illustrates the yield percentages of CO and CH_4 over time for the plasma method using CeO_2/CuO 10% as a catalyst. The experiments were carried out at voltages of 5 kV, 7 kV, and 10 kV, with data collected at 3, 13, and 23 minutes. At 5 kV, the CO yield is around 5%, and the CH_4 yield is approximately 0.5%. At 7 kV, the CO yield is about 10%, with a CH_4 yield of roughly 1%. At 10 kV, the CO yield reaches 24%, and the CH_4 yield is around 3%. The yields remain stable throughout the experiments.

4.2.4. Cerium oxide doped with 20% Copper oxide (CeO_2/CuO 20%)

Figure 33 depicts the percentage of CO_2 conversion over time using the plasma method with a CeO_2/CuO 20% catalyst. Experiments were conducted at three voltages: 5 kV, 7 kV, and 10 kV, with data points recorded at 3 minutes, 13 minutes, and 23 minutes.

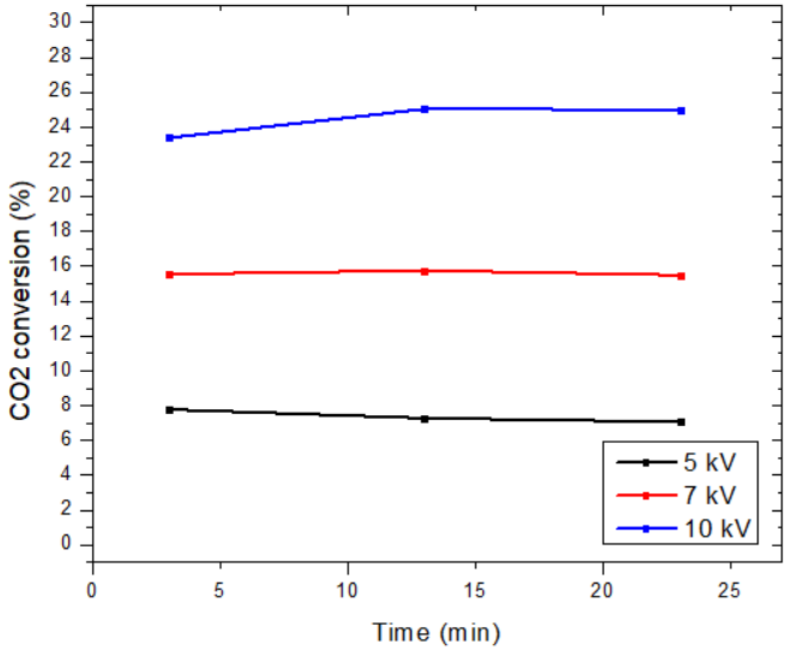

Figure 33: CO_2 conversion at 5, 7, 10 kV with CeO_2/CuO 20% catalyst.

The CO_2 conversion over time is relatively stable in all three voltages. At 5 kV the CO_2 conversion is at 8%, at 7 kV 16% and at 10 kV it fluctuates between 24-26%. The catalyst provides active sites that facilitate the conversion of CO_2. At higher voltages, the energy delivered to the system is increased and so are the reactive species (e.g. radicals, ions) that interact with the catalyst surface. This results in a more stable and efficient conversion. Also, the catalyst can absorb and distribute heat more evenly within the reactor, preventing hot spots and ensuring a more uniform temperature profile. This can lead to more stable reaction rates as the operating conditions remain consistent.

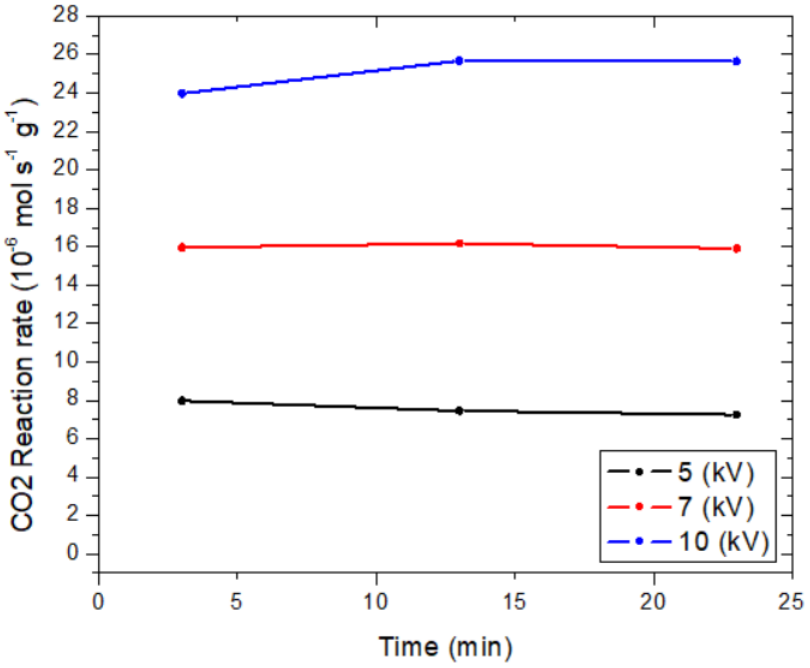

Figure 34. CO_2 reaction rate at 5, 7 and 10 kV with CeO_2/CuO 20% catalyst

Figure 34 shows the CO_2 reaction rate (10^{-6}mol $s^{-1}g^{-1}$) as a function of time (minutes) using CeO_2/CuO 20%. The experiments were conducted at 5,7 and 10 kV and the measurements were taken at 3,13 and 23 minutes.

At 5 kV the CO_2 reaction rate is 8x10^{-6}mol $s^{-1}g^{-1}$, at 7 kV 16x10^{-6}mol $s^{-1}g^{-1}$ and at 10 kV it fluctuates between 24-26x10^{-6}mol $s^{-1}g^{-1}$. The CO_2 reaction rate increases with higher applied voltages. Generally, for all three voltages, the CO_2 reaction rate remains steady over the 23 minutes, indicating that the reaction stabilizes quickly and maintains a consistent rate throughout the experiment.

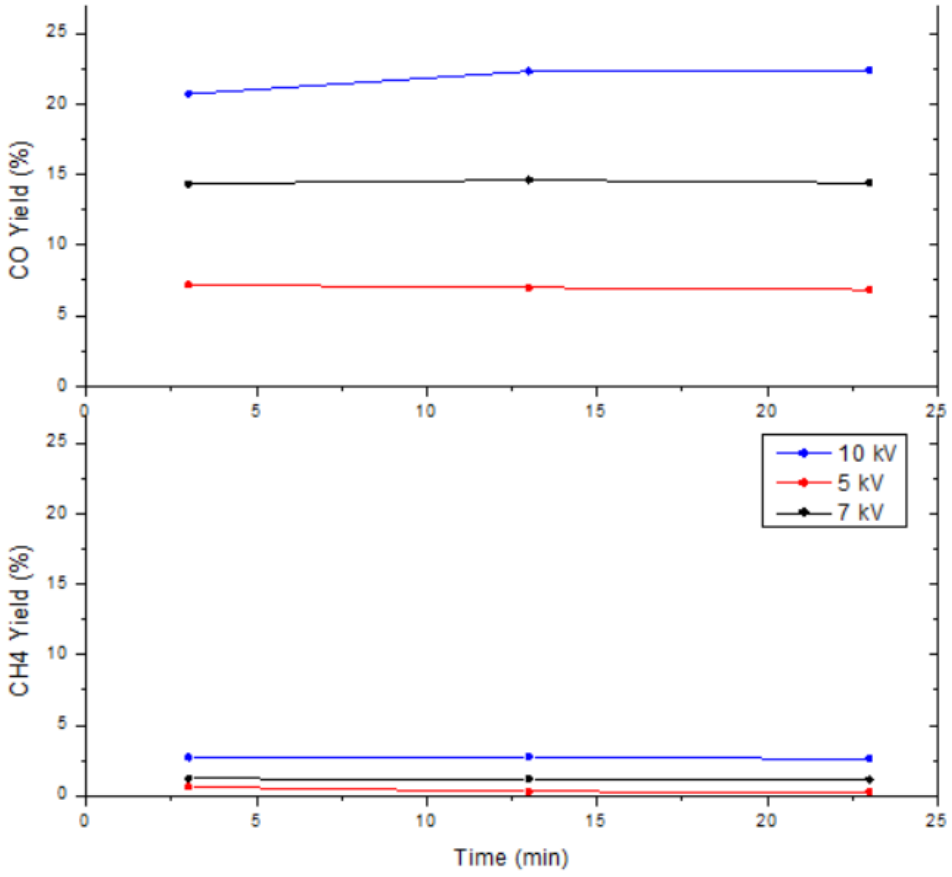

Figure 35. Relationship between CO, CH_4 yield (%) and Temperature (^oC) using a CeO_2/CuO 20% catalyst.

Figure 35 illustrates the yield percentages of CO and CH_4 over time for the plasma method using CeO_2/CuO 20% as a catalyst. The experiments were carried out at voltages of 5 kV, 7 kV, and 10 kV, with data collected at 3, 13, and 23 minutes. At 5 kV, the CO yield is around 7%, and the CH_4 yield is approximately 0.5%. At 7 kV, the CO yield is about 15%, with a CH_4 yield of roughly 1%. At 10 kV, the CO yield reaches 24%, and the CH_4 yield is around 3%. The yields remain stable throughout the experiments.

4.2.5. CO_2 Conversion Comparison Diagrams

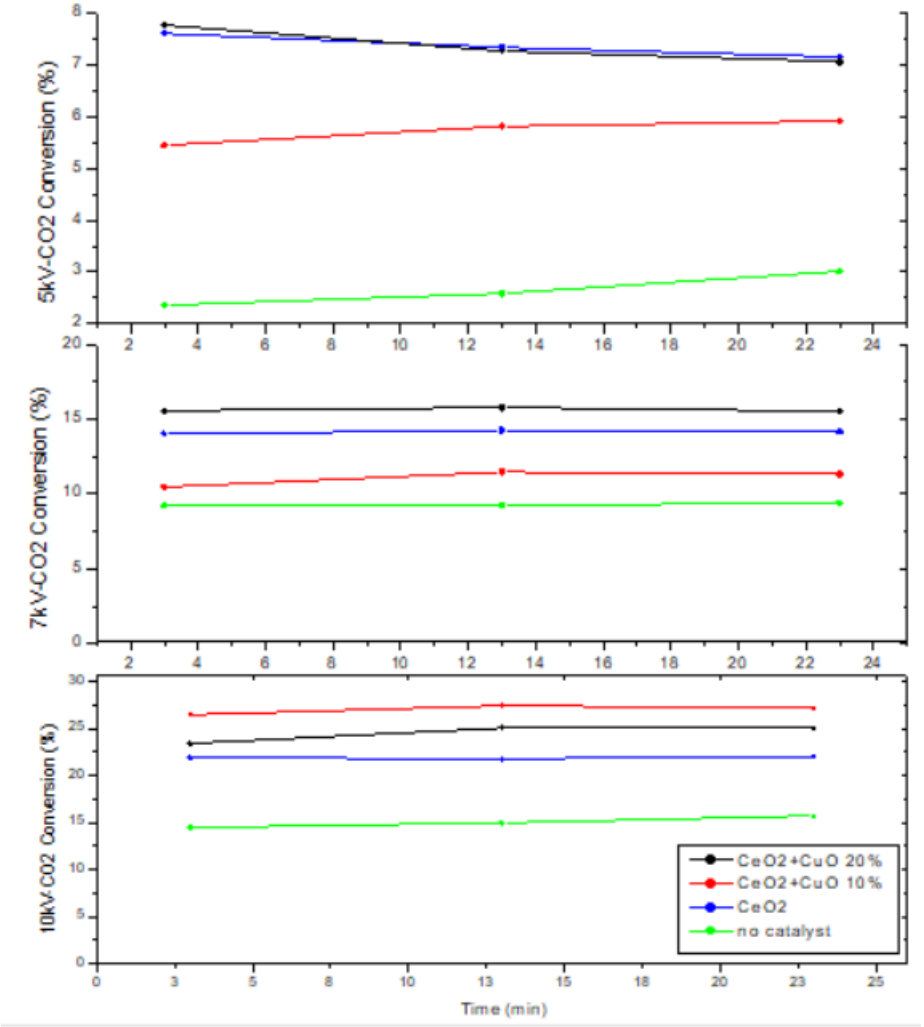

Figure 36: CO_2 conversion (%) for CeO_2, CeO_2/CuO10% and CeO_2/CuO 20% at 5, 7 and 10 kV.

Figure 36 depicts the percentage of CO_2 conversion as a function of time for all three catalysts: CeO_2, CeO_2/CuO 10%, and CeO_2/CuO 20%. Experiments were conducted at three voltages: 5 kV, 7 kV, and 10 kV while the measurements were taken at 3 minutes, 13 minutes, and 23 minutes.

4.2.6. CO_2 Reaction Rate Comparison Diagrams

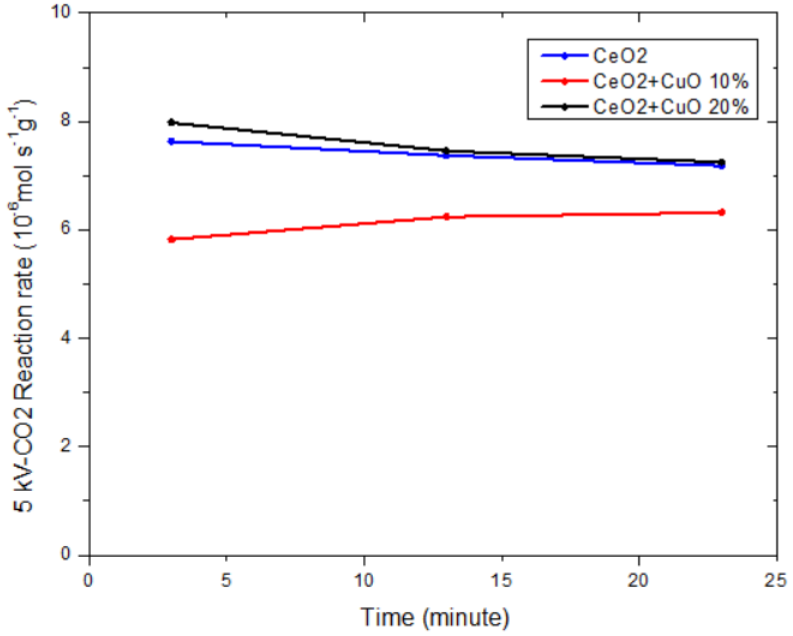

Figure 37: CO_2 reaction rates for CeO_2, CeO_2/CuO10% and CeO_2/CuO 20% at 5kV.

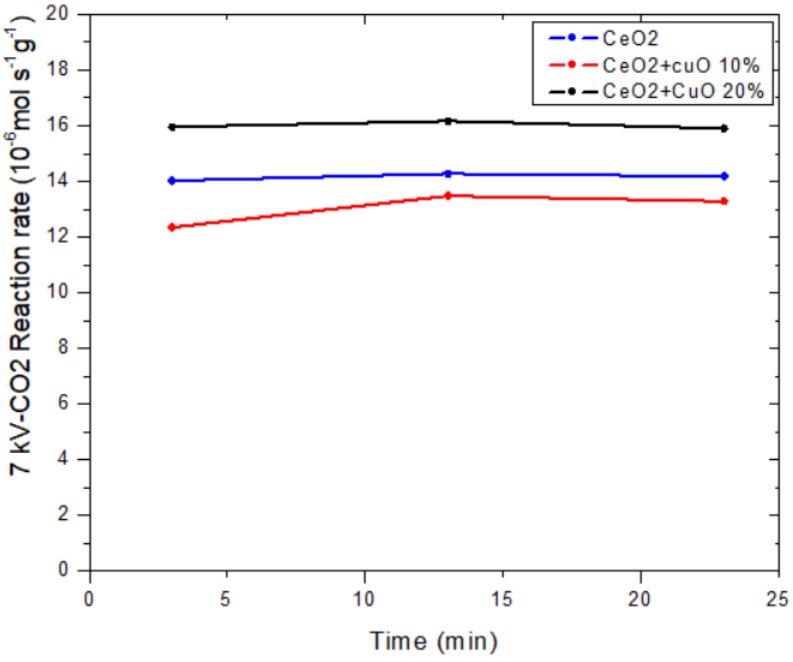

Figure 38: CO_2 reaction rates for CeO_2, CeO_2/CuO10% and CeO_2/CuO 20% at 7 kV.

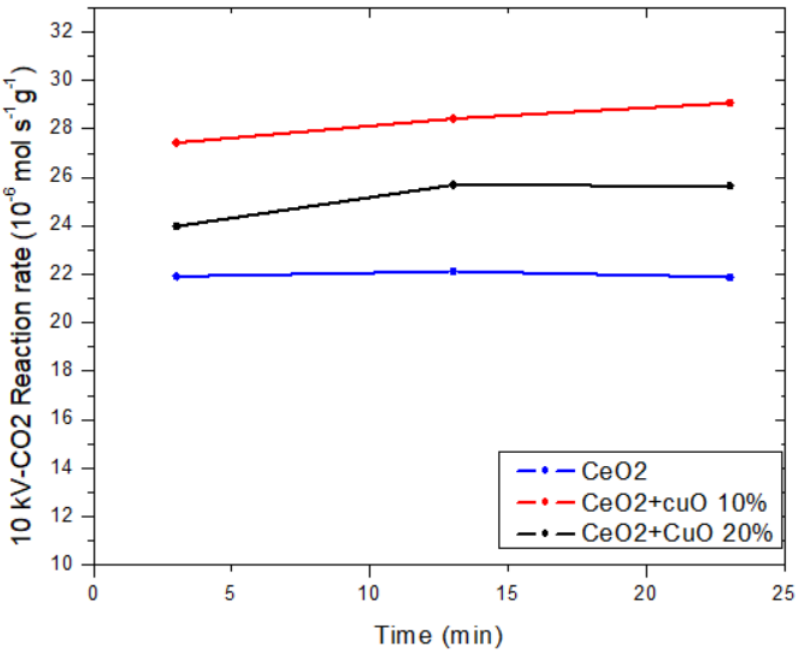

Figure 39: CO_2 reaction rates for CeO_2, CeO_2/CuO10% and CeO_2/CuO 20% at 10 kV.

Figures 37, 38 and 39 illustrate the CO_2 reaction rate (10^{-6}mol $s^{-1}g^{-1}$) over time for the plasma method for 5, 7 and 10 kV. In each diagram, there are all three catalysts except for no catalyst because according to equation (8) this wouldn't be possible as we don't have catalyst mass.

The experiment with no catalyst exhibits the lowest conversion rates and the greatest instability. This highlights the importance of a catalyst, since the catalyst stabilizes plasma and enhances CO_2 conversion.

The experiment with CeO_2 shows a general trend of slight decline at 5 kV, stable performance at 7 kV, and at 10 kV. CeO_2 shows good performance at higher voltages, with stable conversion and reaction rates. More specifically at 5 kV, it is the best-performing catalyst and at 7 kV is the second best catalyst.

The experiment with CeO_2/CuO 10% shows stability across all voltages. At lower voltages the catalyst has the poorest catalytic activity of all, whereas at 10 kV it seems to have the best conversion and reaction rate. This happens because the energy provided at 5 and 7 kV may not be sufficient to fully activate the CuO component in the CeO_2/CuO 10% catalyst. The CuO component requires a certain threshold of energy to effectively

generate reactive oxygen species (ROS) and other active sites that facilitate CO_2 conversion. [42]

Studies have shown that higher energy inputs can lead to increased production of ROS, which are crucial for catalytic processes. [74], [75] At higher voltages (10 kV), the energy provided to the system is significantly higher. This comes with more reactive oxygen species and other active sites hence a more effective activation of the CuO component. At lower voltages, the interaction between CO_2 and the catalyst surface may be less efficient due to insufficient energy to overcome the activation barriers. Additionally, CuO in the CeO_2 matrix can enhance oxygen mobility and increase the number of oxygen vacancies, which are active sites for CO_2 activation. However, this effect is only taking place at higher voltages, where the delivered energy is greater and the CuO component is fully activated. At 10 kV, the synergistic effect between CeO_2 and CuO is maximized, leading to higher CO_2 conversion rates. Research indicates that the presence of CuO can significantly enhance the redox properties of CeO_2, but this requires sufficient energy to exploit these properties effectively. This can lead to lower conversion rates for the CeO_2/CuO 10% catalyst. [70], [76], [77]

Lastly, the experiment with CeO_2/CuO 20% is stable across all voltages, indicating good performance in maintaining CO_2 conversion rates. It demonstrates improved performance and stability compared to pure CeO_2/CuO 10%, CeO_2 and the no-catalyst, with higher conversion rates and more consistent performance over time. CeO_2/CuO 20% shows the best overall performance, maintaining high and stable conversion rates across all voltages.

Using CeO_2/CuO 10% and 20% as catalysts in plasma-based CO_2 hydrogenation can significantly improve conversion efficiency, especially at higher voltages.

The stable conversion rates observed suggest that these catalysts effectively mitigate the instabilities that can occur in plasma reactions, leading to more reliable and efficient CO_2 conversion.

These observations enhance the importance of catalyst composition and optimization in plasma-based CO_2 hydrogenation processes to achieve high and stable conversion efficiencies.

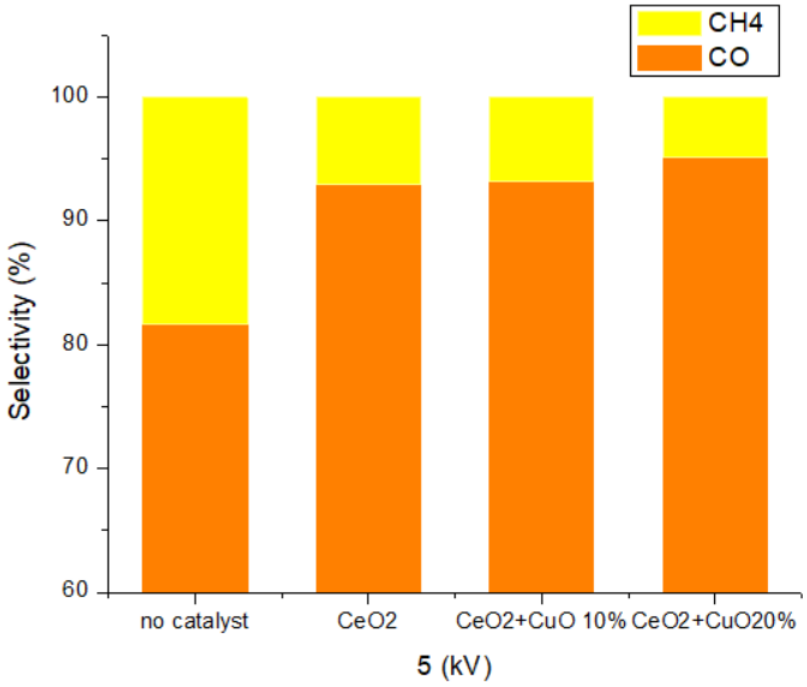

Figure 40. Selectivity (%) for CeO_2, CeO_2/CuO10% and CeO_2/CuO 20% at 5 kV.

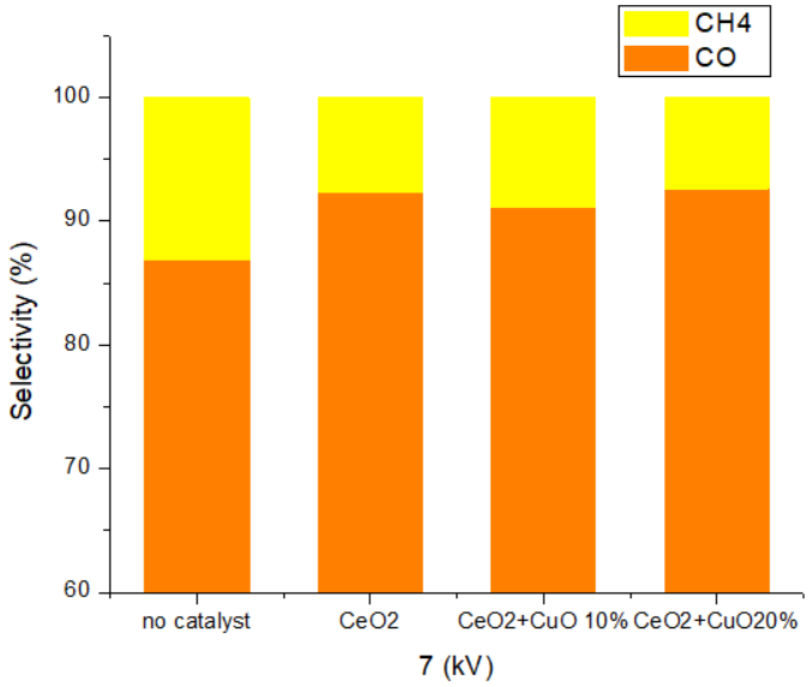

Figure 41. Selectivity (%) for CeO_2, CeO_2/CuO10% and CeO_2/CuO 20% at 7 kV.

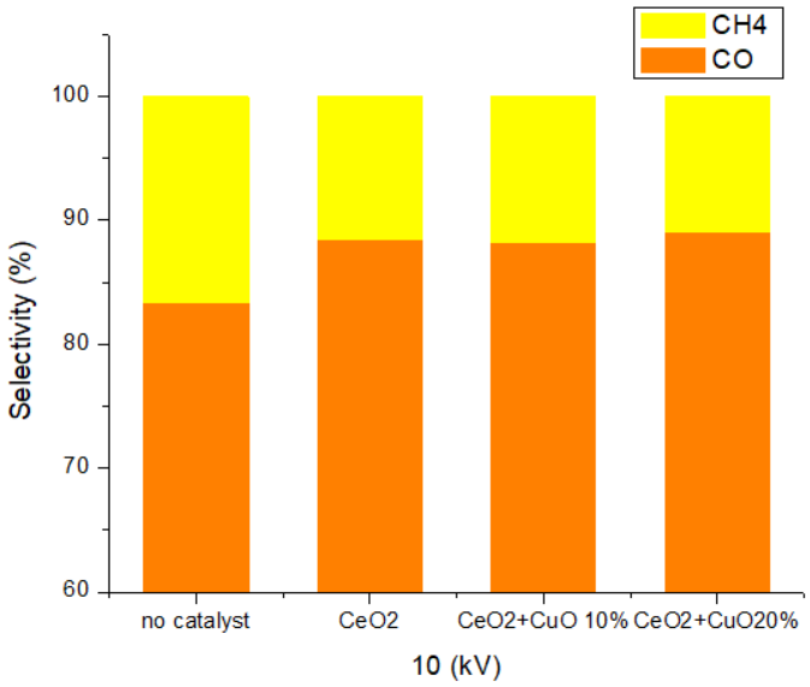

Figure 42. Selectivity (%) for CeO_2, CeO_2/CuO10% and CeO_2/CuO 20% at 10 kV.

Figures 40, 41 and 42 show the selectivity percentages for CO and CH_4 over different catalysts (no catalyst, CeO_2, CeO_2/CuO 10%, and CeO_2/CuO 20%) at three voltages: 5 kV, 7 kV, and 10 kV. For all catalysts and voltages, selectivity for CO remains high (around 85%) compared to CH_4. No catalyst has a relatively high CO selectivity around 83 %. However, the addition of the catalyst in the experiments generally increases the CO selectivity compared to the no-catalyst. CH_4 selectivity is consistently around 15% for all catalysts and voltages, with the no-catalyst control having slightly higher CH_4 selectivity (around 20%). The CO and CH_4 selectivities are not significantly affected by the addition of the CuO component to CeO_2. All three catalysts (CeO_2, CeO_2/CuO 10%, and CeO_2/CuO 20%) show similar selectivity patterns. The higher CO selectivity indicates that CO is the primary product of the CO_2 hydrogenation process under plasma conditions, regardless of the catalyst used.

As mentioned in section 2.1 the hydrogenation reaction can have three products: carbon monoxide, methane and methanol. However, the product is almost only CO. One reason behind this CO-selectivity could be that reaction (1) (reverse water-gas shift, RWGS) is endothermic with a lower enthalpy change (ΔH) of 41.2 kJ/mol compared to the exothermic reactions forming CH_4 and CH_3OH. At higher temperatures, the endothermic

reaction is favored because higher temperatures shift the equilibrium towards products for endothermic reactions (Le Chatelier's principle). [78]

Also, the activation energy for the RWGS reaction is generally lower than that for the methanation or methanol synthesis reactions. This means the RWGS reaction can proceed more readily at the temperatures typically used in plasma reactions. [78] Additionally, the catalysts used (CeO_2, CeO_2/CuO) may have higher selectivity towards the RWGS reaction due to their surface properties and active sites. Cu-based catalysts are known to favor CO formation over CH_4 under certain conditions. [79]

4.3. Stream on time

Stream on time was the last experiment performed, aiming to assess the stability of the best-performing catalyst CeO_2/CuO 20%. The catalyst was firstly reduced with hydrogen (H_2) at 500°C for 2 hours for better catalytic properties.

Following the reduction, the catalyst was tested under plasma conditions at the highest voltage setting of 10 kV. The experiment was conducted for 103 minutes to test the catalyst's stability. The measurements were taken at regular intervals to monitor CO_2 conversion and CO_2 reaction rate.

The results are presented in two graphs: one showing CO_2 conversion (%) over time and the other showing CO_2 reaction rate (10^{-6} mol s^{-1} g^{-1}) over time.

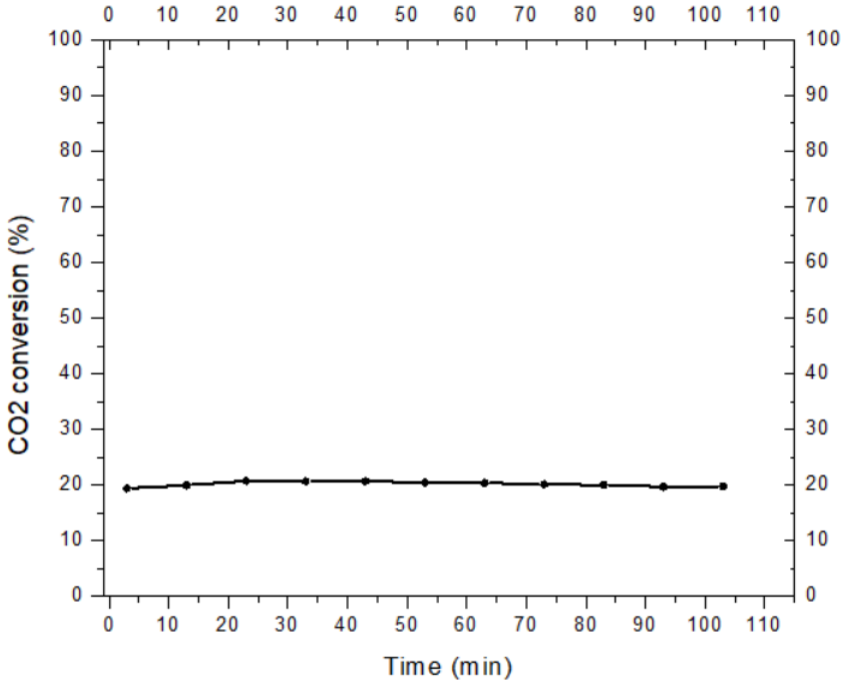

Figure 43. CO_2 conversion (%) for CeO_2/Cu 20% (reduced) at 10 kV

Figure 43 displays CO_2 conversion percentages over time, with measurements taken up to 103 minutes. The CO_2 conversion remains stable at around 20% throughout the experiment, with minor fluctuations.

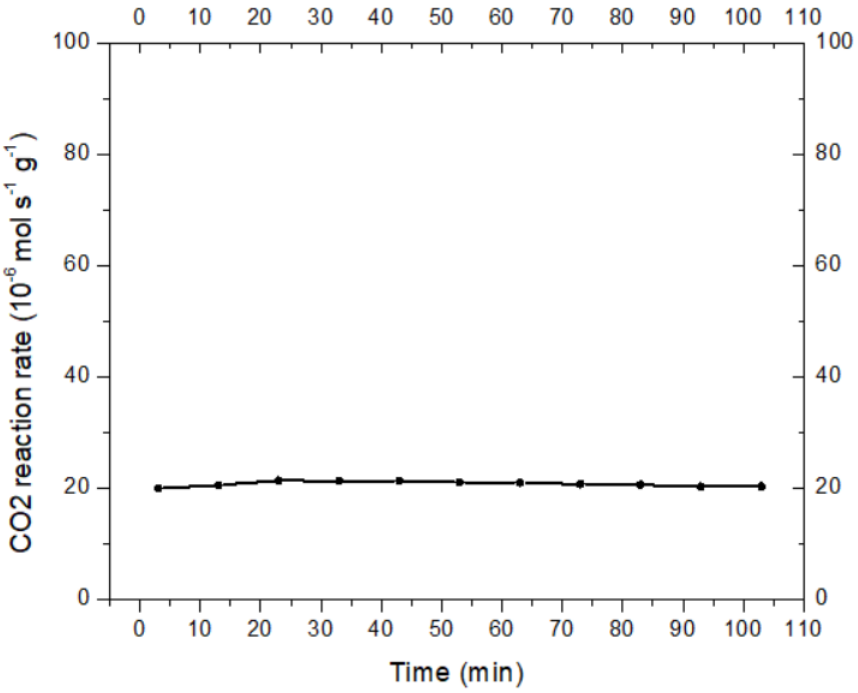

Figure 44. CO_2 reaction rate for CeO_2/Cu 20%(reduced) at 10 kV

Figure 44 shows the CO_2 reaction rate in (10^{-6} mol s^{-1} g^{-1}) over the same time period. The reaction rate remains consistent at approximately 20x10^{-6} mol s^{-1} g^{-1} indicating stable catalytic activity.

The reduction of CeO_2/CuO 20% with H_2 at 500°C is a critical step in activating the catalyst. This process reduces CuO to Cu, which is known to enhance catalytic activity by providing additional active sites for CO_2 hydrogenation.

The stable CO_2 conversion and reaction rate over the 103 minutes demonstrate the catalyst's robustness under high-voltage plasma conditions.

The minor fluctuations observed in the graphs are within an acceptable range and do not indicate significant degradation or deactivation of the catalyst. The CeO_2/CuO 20% catalyst, after reduction with H_2 at 500°C, exhibits excellent stability and performance under plasma conditions at 10 kV. The stable CO_2 conversion and reaction rates over time indicate that the catalyst remains active and effective, making it a promising candidate for sustainable CO_2 hydrogenation applications. This experiment underscores the importance of catalyst preparation and reduction steps in enhancing catalytic properties and ensuring long-term stability.

5. Conclusions

5.1. Hydrogenation of Carbon Dioxide with the Thermal Method

The relationship between CO_2 conversion as well as reaction rate and temperature was demonstrated during the thermal method. Using CeO_2 as a catalyst lead to the hydrogenation reaction taking place after 500°C. Before 500 °C the conversion and the reaction rate were minimal indicating that CeO2 requires high temperature to efficiently convert CO_2.

The addition of the CuO component was crucial for the catalytic performance. Both catalysts CeO_2/CuO 10% and CeO_2/CuO 20% showed a better catalytic performance than pure CeO_2. The reaction in both cases occurred in lower temperatures 400 °C for CeO_2/CuO 10% and 300 °C for CeO_2/CuO 20%. Notably, CeO_2/CuO 20% was the best-performing catalyst since it achieved the highest CO_2 conversion rate. This improved performance is likely due to the synergistic effect of CuO, which offers better adsorption sites and facilitates the reduction process. Research supports the idea that the inclusion of CuO into CeO_2 catalysts significantly boosts their effectiveness in CO_2 hydrogenation. [80]

Additionally, by doping CuO to CeO_2 many oxygen vacancies are created which leads to enhanced catalytic performance. This boosts CO_2 conversion rates at lower temperatures. Research has shown that CeO_2/CuO catalysts exhibit better CO_2 conversion and higher selectivity towards CO due to the enhanced interaction between CeO_2 and CuO, which creates more active sites for the reaction.

To end with, all catalysts favored the formation of CO over CH_4. This happens because of the endothermic nature of the reaction CO_2 to CO under the experimental conditions used. Thermodynamically, CO formation is favored at high temperatures because it is more endothermic, meaning that it absorbs heat. Also, the activation energy of RWGS is smaller than the activation energy of the methanation reaction. This trend can also be found in other research in the literature, where similar behaviors have been observed with other metal-oxide catalysts. [81]

5.2. Hydrogenation of Carbon Dioxide with Plasma

The plasma method exhibited similar catalytic behaviors compared to the thermal method. The CO_2 conversion was stable over time but varied in function of voltage. Higher voltages increased CO_2 conversion, with 10 kV yielding the highest conversion rates. This is the most logical behavior since the greater the energy delivered to a system the higher the conversion rate it will exhibit.

When catalysts were added to the experiments not only did the CO_2 conversion rates across all voltages improve but also the stability of the catalyst did. CeO_2 displayed stable conversion rates over time, with a notable increase in performance at higher voltages. The CeO_2/CuO 10% catalyst showed the lowest conversion rates at 5 kV and 7 kV but significantly improved performance at 10 kV, indicating that higher energy input is necessary for this catalyst to activate effectively. CeO_2/CuO 20% consistently performed well across all voltages, particularly excelling at 10 kV, confirming its superior catalytic properties in plasma conditions. CeO_2/CuO 20% was the best performing catalyst, because even though it did not have the highest conversion rate at 10 kV, it was able to convert the reactants even at low voltages. Plasma conditions create more reactive species and enhance surface reactions, which are critical for effective CO_2 hydrogenation. The CeO_2/CuO 20% catalyst, in particular, demonstrated the highest performance, likely due to the optimal balance of CeO_2 and CuO, which maximizes the availability of active sites and the stability of the catalyst under high-energy conditions.

Product selectivity remained similar to the thermal method, with CO being the predominant product. The presence of CuO in the catalysts enhanced the selectivity towards CO, likely due to its role in facilitating the reduction processes in the plasma environment.

5.3. Comparison of Thermal and Plasma Methods

The thermal and the plasma methods demonstrated a similar behavior when it comes to the efficiency of the catalysts. However, the conditions which the experiments took place need to be considered. Plasma is superior to the thermal method since it can facilitate the hydrogenation reaction at room temperature with similar yields. The plasma method, especially at higher voltages, achieved significant CO_2 conversion without the need for high thermal energy. This could lead to more energy-efficient CO_2 hydrogenation.

Catalyst performance varied between the two methods. CeO_2/CuO 20% was the best-performing catalyst in both methods, its relative performance was more pronounced in the plasma method. This indicates that the plasma environment may enhance the active sites of the catalyst more effectively than thermal energy alone.

The stability tests for the best-performing catalyst, CeO_2/CuO 20%, under plasma conditions at 10 kV, showed stable CO_2 conversion rates over extended periods, confirming the catalyst's durability and suitability for long-term operations in plasma-assisted processes.

In conclusion, this thesis highlights that plasma-assisted CO_2 hydrogenation is a promising approach, offering significant energy savings and effective catalyst utilization compared to traditional thermal methods.

6. Outlook

This study has demonstrated the potential of both thermal and plasma-assisted methods for CO_2 hydrogenation, with significant insights into the performance of CeO_2 and CeO_2/CuO catalysts. The results show that plasma-assisted techniques, especially at higher voltages, provide significant advantages in terms of energy economy and catalytic activity at lower temperatures.

Future study should concentrate on quantifying exactly the CO_2 conversion/energy consumed for both methods. Additionally, optimizing plasma characteristics including voltage and gas flow rates in order to enhance CO_2 conversion and product selectivity.
Detailed research on the interaction of plasma-generated species with catalyst surfaces can provide further information about the mechanisms that drive the reactions.

Exploring new catalyst compositions and synthesis processes can result in the creation of more efficient catalysts. For example, introducing additional metals or oxides within the CeO_2/CuO framework may improve catalytic performance and selectivity.
Advanced characterization techniques, such as in situ spectroscopy and microscopy, can help us understand the structural and electrical properties of these catalysts.

Furthermore, combining plasma-assisted CO_2 hydrogenation processes with renewable energy sources like solar or wind can improve the sustainability and economic viability of these systems. Research into combining renewable energy generation with plasma reactors may open the path for carbon-neutral or even carbon-negative operations.

7. Bibliography

[1] Climate change due to increasing concentrations of carbon dioxide and its impacts on environment in 21st century; a mini review. Kabir, Muhammad. 2023, Journal of King Saud University – Science. https://doi.org/10.1016/j.jksus.2023.102693

[2] Inventory Routing Problem with Carbon Emission Consideration. Aziz, Nur Arina Bazilah BINTI. 2019. 10.11113/matematika.v35.n1.1127

[3] Fundamentals and Catalytic Applications of CeO2-Based Materials. Tiziano Montini, Michele Melchionna, Matteo Monai, and Paolo Fornasiero*. 2016. https://doi.org/10.1021/acs.chemrev.5b00603

[4] The long-run effects of economic, demographic, and political indices on actual and potential CO2 emissions on actual and potential CO2 emissions. Adom, Philip Kofi. 2018, Journal of Environmental Management. https://doi.org/10.1016/j.jenvman.2018.04.090

[5] The long-run effects of economic, demographic, and political indices on actual and potential CO2 emissions. Adom, Philip Kofi. s.l. : Journal Of Environmental Management, 2018. https://doi.org/10.1016/j.jenvman.2018.04.090

[6] Recent advances in catalytic hydrogenation of carbon dioxide. Wang, Wei. 2011, Chemical Society Reviews.

[7] Microwave, Ultrasound, and M
echanochemistry: Unconventional Tools that Are Used to Obtain "Smart" Catalysts for CO2 Hydrogenation, 2018 **https://doi.org/10.3390/catal8070262**

[8] Recent developments in carbon dioxide utilization under mild conditions. SN Riduan, Y Zhang. 2010, Dalton Transactions.

[9] The teraton challenge. A review of fixation and transformation of carbon dioxide. Mikkelsen, Mette. 2010, Energy and Environmental Science.

[10] Global challenges and strategies for control, conversion and utilization of CO2 for sustainable development involving energy, catalysis, adsorption and chemical processing. Song, Chunshan. 2006, Catalysis Today. https://doi.org/10.1016/j.cattod.2006.02.029

[11] Highly active Ni/CeO2 catalyst for CO2 methanation: Preparation and characterization. Ning Rui a b, Xiaoshan Zhang a, Feng Zhang b, Zongyuan Liu b, Xinxiang Cao a, Zhenhua Xie b, Rui Zou a, Sanjaya D. Senanayake b, Yanhui Yang c, José A. Rodriguez b, Chang-Jun Liu a. 2021, Ning Rui a b, Xiaoshan Zhang a, Feng Zhang b, Zongyuan Liu b, Xinxiang Cao a, Zhenhua Xie b, Rui Zou a, Sanjaya D.

Senanayake b, Yanhui Yang c, José A. Rodriguez b, Chang-Jun Liu a. https://doi.org/10.1016/j.apcatb.2020.119581

[12] Enhanced effect of plasma on catalytic reduction of CO2 to CO with hydrogen over Au/CeO2 at low temperature. Zhu, Xiaobing. 2016, Journal of Energy Chemistry 26. https://doi.org/10.1016/j.jechem.2016.11.023

[13] Experimental and kinetic modeling studies of methanol synthesis from CO2 hydrogenation using In2O3 catalyst. Sreetama Ghosh, Joby Sebastian, Louise Olsson, Derek Creaser. 2021, Chemical Engineering Journal. https://doi.org/10.1016/j.cej.2021.129120

[14] The reverse water gas shift reaction: a process systems engineering perspective. Miriam González-Castaño, Bogdan Dorneanu. 2021, Reaction Chemistry & Engineering.

[15] A review of recent catalyst advances in CO2 methanation processes. Jangam Ashok, Subhasis Pati, Plaifa Hongmanorom, Zhang Tianxi, Chen Junmei, Sibudjing Kawi. 2020, Catalysis Today. https://doi.org/10.1016/j.cattod.2020.07.023

[16] Catalysts Europe European Catalyst Manufacturers Association. What are catalysts? [Online]

[17] Hydrogenation of CO2 to formic acid on supported ruthenium catalysts. Cuiying Hao, Shengping Wang. 2011, Catalysis Today. https://doi.org/10.1016/j.cattod.2010.05.034

[18] Catalytic CO2 hydrogenation to formic acid over carbon nanotube-graphene supported PdNi alloy catalysts. Nguyen, Lan Thi Mai. 2015, RSC ADVANCES.

[19] On the activity of supported Au catalysts in the liquid phase hydrogenation of CO2 to formates. Georgy A. Filonenko a b 1, Wilbert L. Vrijburg a, Emiel J.M. Hensen a b, Evgeny A. Pidko. 2016, Journal of Catalysis.

[20] Synthesis of low-cost catalyst NiO(111) for CO2 hydrogenation into short-chain carboxylic acids. Hasan, S.Z. 2020, International Journal of Hydrogen Energy. https://doi.org/10.1016/j.ijhydene.2019.09.102

[21] Fogler, H.S. Elements of Chemical Reaction Engineering 2018.

[22] Rothenberg, Dr. Gadi. Catalysis: Concepts and Green Applications. 2008. DOI:10.1002/9783527621866

[23] RJ Farrauto, L Dorazio, CH Bartholomew. Introduction to catalysis and industrial catalytic processes. 2016.

[24] Room temperature magnetism in CeO 2 —A review. K. Ackland, Jonathon D Coey. 2018. https://doi.org/10.1016/j.physrep.2018.04.002

[25] Ronald M. Heck, Robert J. Farrauto, Suresh T. Gulati. Catalytic Air Pollution Control. 2009. DOI:10.1002/9781118397749

[26] Fundamentals and Catalytic Applications of CeO2-Based Materials. Tiziano Montini, Michele Melchionna, Matteo Monai, and Paolo Fornasiero*. 2016. https://doi.org/10.1021/acs.chemrev.5b00603

[27] Synthesis, Structure and Catalytic Properties of Faceted Oxide Crystals. Xiaohui Zhao, Dr. Mariano D. Susman, Prof. Dr. Jeffrey D. Rimer. 2020. **https://doi.org/10.1002/cctc.202001066**

[28] Fundamentals and Catalytic Applications of CeO2-Based Materials. Tiziano Montini, Michele Melchionna, Matteo Monai, and Paolo Fornasiero*. 2016. https://doi.org/10.1021/acs.chemrev.5b00603

[29] Syntheses and Applications of Noble-Metal-free CeO2-Based Mixed-Oxide Nanocatalysts. Weiting Yang 1 2, Xiao Wang 1, Shuyan Song 1, Hongjie Zhang. s.l. : CHEM, 2019. https://doi.org/10.1016/j.chempr.2019.04.009

[30] Maria Lykaki 1, Sofia Stefa 1. Facet-Dependent Reactivity of Fe2O3/CeO2 Nanocomposites: E_ect of Ceria Morphology on CO Oxidation. 2019. 10.3390/catal9040371

[31] On the structure dependence of CO oxidation over CeO2 nanocrystals with well-defined surface planes. Wu, Zili. s.l. : Journal of Catalysis, 2012. https://doi.org/10.1016/j.jcat.2011.09.011

[32] Effect of the Preparation Method on the Physicochemical Properties and the CO Oxidation Performance of Nanostructured CeO2/TiO2 Oxides. **https://doi.org/10.3390/pr8070847**

[33] Hydrothermal Synthesis of ZnO–doped Ceria Nanorods: Effect of ZnO Content on the Redox Properties and the CO Oxidation Performance. Sofia Stefa 1, Maria Lykaki 1,Vasillios Binas 2,Pavlos K. Pandis 3,Vassilis N. Stathopoulos andMichalis Konsolakis. s.l. : 10th Anniversary of Applied Sciences-Invited Papers in Chemistry Section), 2020. **https://doi.org/10.3390/app10217605**

[34] Facet-Dependent Reactivity of Fe2O3/CeO2 Nanocomposites: Effect of Ceria Morphology on CO Oxidation. Maria Lykaki, Sofia Stefa. 2019. **https://doi.org/10.3390/catal9040371**

[35] Doped apatite-type lanthanum silicates in CO oxidation reaction. Pavlos K. Pandis, Dimitris E. Perros, Vassilis N. Stathopoulos. s.l. : Catalysis Communication, 2018. https://doi.org/10.1016/j.catcom.2018.06.017

[36] Unveiling the reaction pathway on Cu/CeO2 catalyst for electrocatalytic. Xue, Lei. s.l. : Applied Catalysis B: Environmental , 2022. https://doi.org/10.1016/j.apcatb.2021.120951

[37] Study of Catalytic Activity at the CuO−CeO2 Interface for CO Oxidation. Ai-Ping Jia, Shi-Yu Jiang, Ji-Qing Lu*, and Meng-Fei Luo. 2010.

[38] CuO/CeO2 catalysts: Redox features and catalytic behaviors. Xiaolan Tang, Baocai Zhang, Yong Li, Yide Xu, Qin Xin, Wenjie Shen. s.l. : Applied Catalysis A: General, 2005.

[39] Carbonate-mediated Mars–van Krevelen mechanism for CO oxidation on cobalt-doped ceria catalysts: facet-dependence and coordination-dependence. Liu, Bing. s.l. : Physical Chemistry Chemical Physics.

[40] Sequencing the Cuox Active Species for Co Preferential Oxidation at Low-Temperature Over Ceo2-Cuo Compo Low-temperature CO oxidation on CuO-CeO2-ZrO2 catalysts prepared by a facile surfactant-assisted grinding method. Hu, Xuan. 2023.site Catalysts. Wang, Qi. 2022.

[41] Unveiling the reaction pathway on Cu/CeO2 catalyst for electrocatalytic. Xue, Lei. s.l. : Applied Catalysis B: Environmental , 2022. https://doi.org/10.1016/j.apcatb.2021.120951

[42] MOF-derived high oxygen vacancies CuO/CeO2 catalysts for low-temperature CO preferential oxidation. Fen Liu a, Xiaohua Chen a, Weiwei Jie. 2024. https://doi.org/10.1016/j.jcis.2024.06.110

[43] Generation and Applications of Plasma (An Academic Review). Mehmood, Faizan. 2018. doi: 10.20944/preprints201810.0061.v1

[44] The long-run effects of economic, demographic, and political indices on actual and potential CO2 emissions. Adom, Philip Kofi. s.l. : Journal Of Environmental Management, 2018. https://doi.org/10.1016/j.jenvman.2018.04.090

[45] Non-thermal plasma catalysis for CO2 conversion and catalyst design for the process . 23, s.l. : Journal of Physics D: Applied Physics, 2021, Vol. 54. **DOI** 10.1088/1361-6463/abe9e1

[46] The teraton challenge. A review of fixation and transformation of carbon dioxide. Mikkelsen, Mette. 2010, Energy and Environmental Science.

[47] Catalytic CO2 hydrogenation to formic acid over carbon nanotube-graphene supported PdNi alloy catalysts. Nguyen, Lan Thi Mai. 2015, RSC ADVANCES.

[48] On the activity of supported Au catalysts in the liquid phase hydrogenation of CO2 to formates. Georgy A. Filonenko a b 1, Wilbert L. Vrijburg a, Emiel J.M. Hensen a b, Evgeny A. Pidko. 2016, Journal of Catalysis.

[49] Facet-Dependent Reactivity of Fe2O3/CeO2 Nanocomposites: Effect of Ceria Morphology on CO Oxidation. Maria Lykaki, Sofia Stefa. 2019. **https://doi.org/10.3390/catal9040371**

[50] A review of the advances in catalyst modification using nonthermal plasma: Process, Mechanism and Applications. Zhiping Ye a b f, Liang Zhao a, Anton Nikiforov. s.l. : Advances in Colloid and Interface Science, 2022, Vol. 308. https://doi.org/10.1016/j.cis.2022.102755

[51] Low-temperature plasma synthesis of carbon nanotubes and graphene based materials and their fuel cell applications. Qi Wang, a Xiangke Wang,*ab Zhifang Chai*b and Wenping Hu*c. s.l. : Chemical Society Reviews, 2013.

[52] A review of non-thermal plasma -catalysis: The mutual influence and sources of synergetic effect for boosting volatile organic compounds removal. Nacer Belkessa a, Aymen Amin Assadi. s.l. : Environmental Research, 2024. https://doi.org/10.1016/j.envres.2024.119333

[53] Removal of low-concentration formaldehyde in air by DC corona discharge plasma. Yajuan Wan, Xing Fan, Tianle Zhu. s.l. : Chemical Engineering Journal, 2011, Vol. 171. https://doi.org/10.1016/j.cej.2011.04.011

[54] Characteristics of Gliding Arc Discharge Plasma. Lin Lie, Wu Bin. 2006. **DOI** 10.1088/1009-0630/8/6/06

[55] A uniform glow discharge plasma source at atmospheric pressure. Moon, Se Youn, Choe, W. and Kang, B. K. 2004. https://doi.org/10.1063/1.1639135

[56] Non-Thermal Plasma Incorporated with Cu-Mn/γ-Al2O3 for Mixed Benzene Series VOCs' Degradation. Zhu, Yifan. s.l. : Progress in Plasma-Assisted Catalysis for Green Energy Production and Environmental Application, 2023. **https://doi.org/10.3390/catal13040695**

[57] Volatile organic compounds (VOCs) removal in non-thermal plasma double dielectric barrier discharge reactor. Mustafa, Muhammad Farooq. 2018. https://doi.org/10.1016/j.jhazmat.2018.01.021

[58] Dielectric-Barrier Discharges: Their History, Discharge Physics, and Industrial Applications. Kogelschatz, Ulrich. 2003.

CO2 dissociation in a packed bed DBD reactor: First steps towards a. Michielsen, I. s.l. : Chemical Engineering Journal, 2017.

[60] Non-thermal plasma technology for the conversion of CO2. Bryony Ashford, Xin Tu. s.l. : Current Opinion in Green and Sustainable Chemistry, 2017. https://doi.org/10.1016/j.cogsc.2016.12.001

[61] About the development of single microdischarges in dielectric barrier discharges in CO2 and CO2/N2 gas mixtures. Brandenburg, Ronny. s.l. : European Physical Journal Special Topics, 2017.

[62] A Review of CeO2 Supported Catalysts for CO2 Reduction to CO through the Reverse Water Gas Shift Reaction. Ebrahimi, Parisa. 2022. **https://doi.org/10.3390/catal12101101**

[63] Facet-Dependent Reactivity of Ceria Nanoparticles Exemplified by CeO2-Based Transition Metal Catalysts: A Critical Review. Michalis Konsolakis, Maria Lykaki. s.l. : Commemorative Issue in Honor of Professor Gerhard Ertl on the Occasion of His 85th Birthday), 2021. **https://doi.org/10.3390/catal11040452**

[65] A review on the catalytic conversion of CO2 using H2 for synthesis of CO, methanol, and hydrocarbons. Tesfalem Aregawi Atsbha a, Taeksang Yoon a, Park Seongho. s.l. : Journal of CO2 Utilization, 2021, Vol. 44. https://doi.org/10.1016/j.jcou.2020.101413

[66] CO 2 Hydrogenation to Methanol Over Cu/ZnO/Al 2 O 3 Catalyst: Kinetic Modeling Based on Either Single-or Dual-Active Site Mechanism. Li, Hou-Xing. 2022. DOI:10.1007/s10562-021-03913-0

[67] Catalytic Hydrogenation of CO2 over Ni-Based Catalysts in a Fixed-Bed Reactor. Lee. s.l. : Journal of CO2 Utilization , 2019.

[68] Plasma-Assisted CO2 Hydrogenation on Metal-Oxide Catalysts. Smith. s.l. : Applied Ctalysis B: Environmental, 2020.

[69] A facile method for the preparation of ceramic beads with hierarchical porosity. Vasiliki Chalkia, V. N. Stathopoulos. s.l. : Ceramics International, 2017. https://doi.org/10.1016/j.ceramint.2017.09.102

[70] Plasma–liquid interactions: a review and roadmap. Bruggeman, P J. s.l. : Plasma Sources Science and Technology, 2016. **DOI** 10.1088/0963-0252/25/5/053002

[71] Fluid modelling of a packed bed dielectric barrier discharge plasma reactor. Bogaerts, Van Laer &. s.l. : Plasma Sources Science and Technology, 2016. **DOI** 10.1088/0963-0252/25/1/015002

[72] Plasma Technology: An Emerging Technology for Energy Storage. s.l. : ACS Energy Letters, 2018. https://doi.org/10.1021/acsenergylett.8b00184

[73] A review on the catalytic conversion of CO2 using H2 for synthesis of CO, methanol, and hydrocarbons. Tesfalem Aregawi Atsbha a, Taeksang Yoon a, Park Seongho. s.l. : Journal of CO2 Utilization, 2021, Vol. 44. https://doi.org/10.1016/j.jcou.2020.101413

[74] Plasma-Enabled Dry Methane Reforming. Zunrong Sheng, Seigo Kameshima, Kenta Sakata and Tomohiro Nozaki. s.l. : Plasma Chemistry and Gas Conversion, 2018. DOI: 10.5772/intechopen.80523

[75] Biogas Reforming to Syngas: A Review. Zhao, Xianhui. 2020. https://doi.org/10.1016/j.isci.2020.101082

[76] Fluid modelling of a packed bed dielectric barrier discharge plasma reactor. Bogaerts, Van Laer &. s.l. : Plasma Sources Science and Technology, 2016. **DOI** 10.1088/0963-0252/25/1/015002

[77] Plasma Technology: An Emerging Technology for Energy Storage. s.l. : ACS Energy Letters, 2018. https://doi.org/10.1021/acsenergylett.8b00184

[78] Lower, Stephen. Le Chatelier's Principle - Thermodynamic Considerations:.

[79] The role of copper in Low-Temperature Method synthesis catalysts: a review. A. Karelovic, P. Ruiz. s.l. : Catalysis Science & Technology, 2015.

[80] Kinetics of the Reverse Water-GAs shift reaction over Ni/Al2O3 Catalyst. Rognerud. s.l. : Industrial & Engineering Chemistry Research, 2018. **https://doi.org/10.1002/cjce.22370**

[81] The role of copper in Low-Temperature Method synthesis catalysts: a review. A. Karelovic, P. Ruiz. s.l. : Catalysis Science & Technology, 2015.